Geomorphology 502 (2026) 110264

Contents lists available at ScienceDirect

Geomorphology

journal homepage: www.journals.elsevier.com/geomorphology

# Large rock slope deformations: Evidence of orogen-scale distribution from an original inventory in central Apennines (Italy)

E. Di Luzio [a,d], M. Saroli [b,c,d], M. Moro [d], E. Zullo [b,d,*], M. Albano [d], G. Scarascia Mugnozza [e], M.E. Discenza [f], M. Fiorucci [b,c], D. Guglietta [a], C. Esposito [e]

[a] CNR-IGAG, Consiglio Nazionale delle Ricerche, Istituto di Geologia Ambientale e Geoingegneria, Montelibretti, Via Salaria Km 29.3, Monterotondo St., 00165, Rome, Italy
[b] DICeM-Dipartimento di Ingegneria Civile e Meccanica dell'Università degli Studi di Cassino, Via G. di Biasio 43, 03043, Cassino, Italy
[c] European University of Technology, EUt+, European Union, via G. di Biasio 43, 03043, Cassino, Italy
[d] Istituto Nazionale di Geofisica e Vulcanologia, Via di Vigna Murata 605, 00143, Rome, Italy
[e] "Sapienza" University of Rome, Department of Earth Sciences and Research, Centre for Geological Risks (CERI), Piazzale Aldo Moro 5, 00185, Rome, Italy
[f] Geoservizi S.r.l., Via Luigi e Nicola Marinelli, 2, 86025, Ripalimosani, Italy

ARTICLE INFO

*Keywords:*
Deep-seated gravitational slope deformation
Regional inventory
Statistical analysis
Central Apennines

ABSTRACT

Large rock slope deformations, widely known as Deep-Seated Gravitational Slope Deformations (DSGSDs), are widespread in mountain regions worldwide, yet a comprehensive understanding of their occurrence and distribution remains a complex task. This work presents an inventory of 337 DSGSDs documented in the central Apennines (Abruzzi region, Italy). The dataset was implemented with case histories from former studies and completed after a five-year-long photointerpretation work, combined with field checks. About 260 new sites were documented.

DSGSDs morphometric parameters, including areal extent and morphology of the hosting rock slopes, were investigated through statistical analyses. A threshold value of 1 $km^2$ marks the limit of a power law behaviour for the frequency-size distribution of large rock slope deformations. Geospatial analysis reveals significant linear clustering along inherited tectonic lineaments, including Mio-Pliocene thrusts and Plio-Quaternary normal faults. Geolithological conditions also influence DSGSDs spatial distribution and size, as the largest gravity-driven deformations, with areas exceeding 4 $km^2$, are located along thrusts and collapsed backlimbs within carbonate platform sequences.

Although structural features and lithology may be regarded as the prevailing conditioning factors, the long-term evolution of the belt, characterized by multi-step thrusting and related uplift, and the bulk topography of the region seem to have played an important role. Apart from linear clustering, the late Messinian portion of the belt presents better conditions for DSGSDs development in terms of localized uplift, local relief, average altimetric range, and slope roughness.

Finally, comparison to an inventory from the confining Molise region outlined similar DSGSDs spatial frequency and morphometric values, thus evidencing a homogenous signature in the central Apennine for this kind of geological process. Results of this study provide a basis for further research to unravel the morphogenetic significance of large rock slope deformations in landscape evolution.

## 1. Introduction

Gravitational deformations involving large portions of mountain slopes are recognized through the spatial association of geomorphological diagnostic features. Double ridges, trenches, grabens, scarps, and counterscarps in the upper and middle slope sections are combined with increased rock fracturing, bulging, and landslides in the lower sectors (Radbruch-Hall, 1978; Bovis, 1982; Savage and Varnes,

* Corresponding author at: DICeM-Dipartimento di Ingegneria Civile e Meccanica dell'Università degli Studi di Cassino, Via G. di Biasio 43, 03043, Cassino, Italy.
*E-mail addresses:* emiliano.diluzio@igag.cnr.it (E. Di Luzio), michele.saroli@unicas.it (M. Saroli), marco.moro@ingv.it (M. Moro), enrica.zullo@unicas.it, enrica.zullo@ingv.it (E. Zullo), matteo.albano@ingv.it (M. Albano), gabriele.scarasciamugnozza@uniroma1.it (G. Scarascia Mugnozza), discenza@geoservizisrl.net (M.E. Discenza), matteo.fiorucci@unicas.it (M. Fiorucci), daniela.guglietta@igag.cnr.it (D. Guglietta), carlo.esposito@uniroma1.it (C. Esposito).

https://doi.org/10.1016/j.geomorph.2026.110264
Received 11 November 2025; Received in revised form 13 February 2026; Accepted 2 March 2026
Available online 3 March 2026

1987; Chigira, 1992; Agliardi et al., 2001, 2012; Ambrosi and Crosta, 2006, 2011; Jaboyedoff et al., 2013; Discenza and Esposito, 2021). Moreover, these geological processes are characterized by small displacements compared to their size and very low deformation rates, in the order of mm/yr or exceptionally cm/yr (Saroli et al., 2005; Moro et al., 2009, 2011; Frattini et al., 2013; Jaboyedoff et al., 2013; Pánek and Klimeš, 2016; Stramondo et al., 2016; Delchiaro et al., 2021; Albano et al., 2023). Although scholars share these general concepts, nomenclature is still a matter of debate, as different definitions are being used.

The term Deep-Seated Gravitational Slope Deformation, first introduced by Malgot (1977), is nowadays largely used with the acronym DSGSD (Dramis and Sorriso-Valvo, 1994; Crosta, 1996; Agliardi et al., 2001). DSGSD refers to a gravity-driven process with a considerable depth (tens to hundreds of meters) of the rock mass volume under deformation over the stable bedrock. However, since subsurface information is rare, the concepts of thickness or depth should be disregarded as a general criterion. Although a literature review is not among the objectives of this work (see Discenza and Esposito, 2021 for a thorough revision), other descriptions can be mentioned that underline different and important aspects. For instance, the term "Mass Rock Creep" (e.g. Radbruch-Hall, 1978; Chigira, 1992) focuses on the mechanical, time-dependent behaviour of involved rock masses, whereas the concept of "Slope Tectonics" (Jaboyedoff et al., 2011) evidences the role of local, topographic stress fields in driving deformations. On the other hand, Jarman (2006) and Jarman and Harrison (2019) introduced the definition "Rock Slope Deformation" (RSD), applied to a bedrock mass that has lost its structural integrity, being affected by a downslope gravitational movement and merging laterally with undeformed slope areas, without necessarily sharp boundaries.

"Large rock slope deformation", or LRSD, may be a very convincing definition and comes close to an efficient description of the phenomenon. On the other hand, DSGSD is an acronym widely used in the scientific literature and introducing a new one would add confusion. Therefore, we kept the term DSGSD but referring it to indicate a large rock slope deformation: i) involving wide areas of rock slopes with planar dimensions in the order of hundreds of meters to few kilometers; ii) showing typical geomorphological features distributed from the top of a mountain ridge to the piedmont zone; iii) potentially capable to modify the original structural asset of the hosting rock slope; iv) characterized by both narrow or diffuse lateral margins, not necessarily with a head scarp; and v) delimited at an unknown depth by a continuous or discontinuous deformation surface/zone associated with creep dynamics.

In accordance with the increasing scientific interest in DSGSDs, regional databases were implemented in the European Alps (Agliardi et al., 2013; Crosta et al., 2013), the Eastern Pyrenees (Jarman et al., 2014), the Scottish Highlands (Jarman, 2006), the British Mountains (Jarman and Harrison, 2019) and the Western Carpathians (Pànek et al., 2019). Outside Europe, DSGSDs inventories were completed in Japan (Kaneda and Kono, 2017), New Zealand (McLean et al., 2015) and Taiwan (Tsou et al., 2015). Based on these works, efforts to produce a global inventory were recently undertaken (Toločka, 2025).

For the central Apennines, inventories of large rock slope deformation were compiled in a technical, public landslide database (IFFI, 2007). Only recently, the Italian Geological Map (CARG Project) at 1:50,000 scale began reporting a few isolated case histories (https://www.isprambiente.gov.it/Media/carg). However, several papers published in the last four decades on single DSGSD within the region (e.g. Crescenti et al., 1987; Dramis et al., 1987; Di Luzio et al., 2004a, 2022; Martino et al., 2004; Galadini, 2006; Scarascia Mugnozza et al., 2006; Esposito et al., 2007, 2013, 2014, 2021; Moro et al., 2009, 2012; Bianchi Fasani et al., 2011, 2014; Discenza et al., 2011, 2023a; Gori et al., 2014; Albano et al., 2015; Della Seta et al., 2017; Del Rio et al., 2021; Khalaf et al., 2025), demanded an updated scientific review and an original investigation.

The lack of regional mapping is critical from a scientific perspective. Furthermore, DSGSDs inventories must be considered for effective hazard and risk assessment in the study area. Generally, in central Apennines mass wasting and sediment flux are limited from observed DSGSD areas or along their bordering channels. Nevertheless, rapid landslide events of small to moderate dimensions can enhance the volume of transported material (e.g. Di Luzio et al., 2021). In a few sites, Apennine DSGSDs evolved in large rock avalanches (Di Luzio et al., 2004b; Scarascia Mugnozza et al., 2006; Bianchi Fasani et al., 2014), i.e. formative events which can change valley floors topography and deliver hundreds or even thousands of cubic meters of clastic material in a short time, thus posing a serious threat in terms of hydrogeological risk.

Therefore, the main objective of this work was the realization of an original DSGSDs inventory for the axial zone of the central Apennine belt included within the territory of the Abruzzi region (Fig. 1). A morphological criterion was adopted, drawing boundaries of each DSGSD polygon to encompass distinguishing geomorphological features (Fig. 2a–g). Following the distinction from Jarman (2006), the inventory does not include short-travelled translational slides, in which the structural asset of the rock mass is partially maintained, and both head scarps and lateral boundaries are evident. DSGSDs morphometric parameters and slope morphological variables for the whole dataset were calculated.

To gain a deeper understanding of factors controlling the onset and development of large rock slope deformations, a further aim of the research was to compare the distribution of DSGSDs, the regional lithological framework, the trend of the inherited main structural features, and the location of the active fault network. Moreover, similarly to other regions (e.g. Agliardi et al., 2013), this paper tried to frame the characteristics of the DSGSD inventory within the long-term evolution of the mountain belt and the bulk topography of the orogen, and to investigate the morphogenetic role of DSGSDs at a local scale.

Finally, this work follows the paper by Discenza et al. (2023b), who completed a similar inventory in the nearby Molise region, and it represents a further piece of the ambitious attempt to complete a DSGSD dataset of the entire Apennine belt.

## 2. Geological and morphotectonic setting

The central Apennines formed through the deformation of a Meso-Cenozoic sedimentary wedge during the convergence between the African (Adriatic) and European plates (e.g. Doglioni, 1991; Gueguen et al., 1998; Carminati and Doglioni, 2012). In the pre-orogenic context, from the Triassic to the Paleogene, different paleogeographic domains originated because of Early Jurassic extensional tectonics, which locally drowned former shallow-water carbonate platforms and coastal environments.

Successively, between the Late Miocene and the Early Pleistocene, sedimentary environments were incorporated into a belt-foredeep-foreland system migrating NE-wards (e.g. Malinverno and Ryan, 1986; Patacca and Scandone, 1989; Cosentino et al., 2010; Vezzani et al., 2010). The architecture of the belt is characterized by NW-SE-trending and NE-verging thrusts enucleating at upper or middle crustal levels (Billi et al., 2006; Patacca et al., 2008; Di Luzio et al., 2009). Main thrusts separate different geolithological domains (GLD): the Simbruini and Marsica platforms on the west, the slope-to-basin sequences of the Gran Sasso-Genzana-La Queglia domains in the central sectors, and the Apulian platforms units on the east and south-east of the region (Maiella, Morrone-Porrara, Pizzalto, Rotella ridges). Along the eastern regional boundary, the Apulian structures are tectonically overridden by the Molise nappe. These are made of a deep-basin geological sequence and characterized by foredeep deposits with a larger clayey fraction with respect to the flysch lithotypes in the central and northern areas (Fig. 3). Geological domains were firstly incorporated in the Apennine belt between the Late Tortonian and the Middle Pliocene (Fig. 3, upper right insight), thus experiencing differentiate long term history in terms of uplift, rock deformation and damage. Further localized deformation was

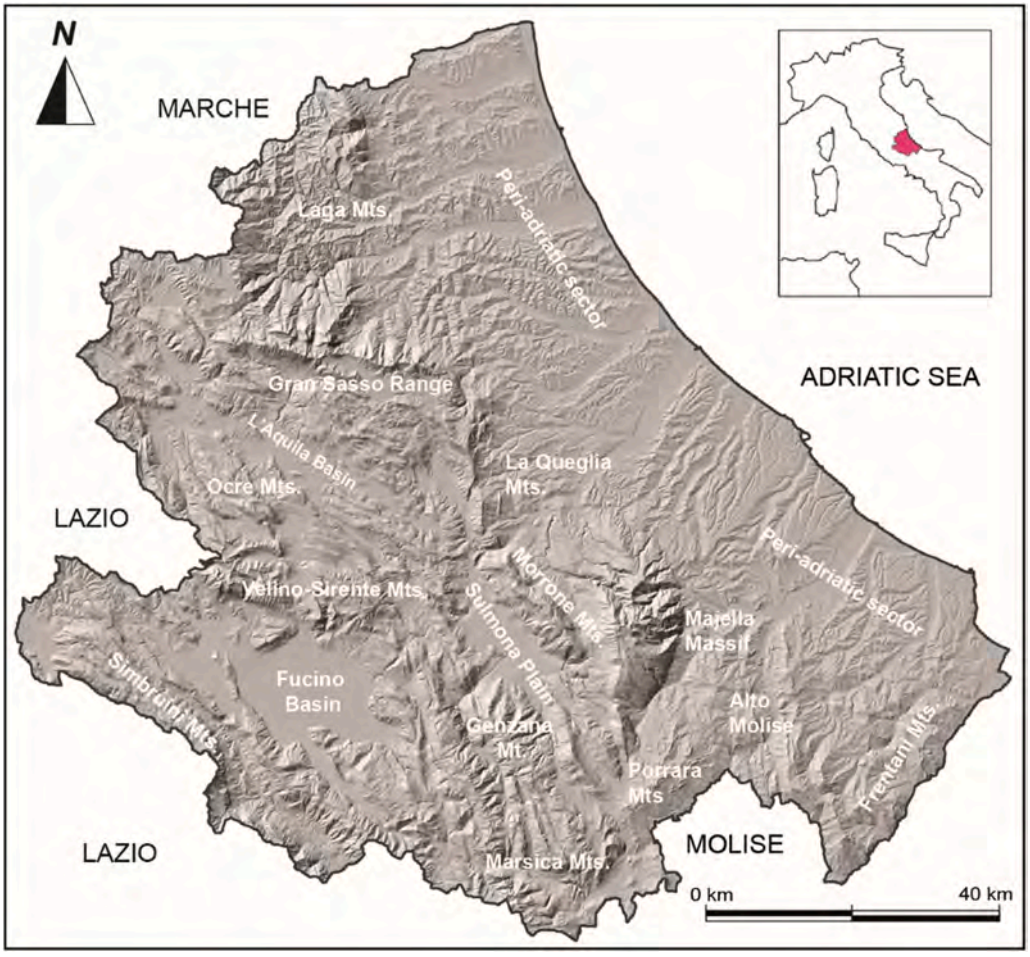


**Fig. 1.** Hillshade imaged of the Abruzzi region derived from NASA Shuttle Radar Topography (SRTM, 30 m). Main mountain areas and intramontane basin are reported.

determined by out-of-sequence, deep stacking processes involving the Permo-Triassic section of the Apennine wedge during the Pleistocene, which were responsible for the passive uplift of roof units in the stacked sedimentary nappes (Fig. 4a).

Since the Late Tortonian, renewed extensional tectonics followed the compressional wave, dissecting the thrust edifice (e.g. Patacca et al., 1990; Faccenna et al., 1996; Cavinato and De Celles, 1999). During the Middle and Late Pliocene, normal faulting increased and shifted towards the axial zone of the belt, at that time characterized by a low-relief continental environment (e.g. Galadini and Messina, 1994; Galadini et al., 2003). Large tectonic depressions began to open as the Fucino, Sulmona, and L'Aquila basins (Fig. 3); the Plio-Quaternary evolution of extensional basins and active faulting has been extensively studied in central Apennines (e.g. Galadini and Galli, 2000; Cavinato et al., 2002; Galli et al., 2008; Gori et al., 2017). Afterwards, since the end of the Early Pleistocene, local normal faulting was accompanied by a dome-like uplift of the whole region, with uplift rates ranging between 0.3 and 1 mm/yr (Ambrosetti et al., 1982; Dramis, 1992; D'Agostino et al., 2001; Bartolini et al., 2003; Centamore and Nisio, 2003; Pizzi, 2003). The uplift process brought to relief rejuvenation and increased linear erosion, these factors controlling the morphodynamics of slopes (Bianchi Fasani et al., 2014; Della Seta et al., 2017).

During Quaternary, unlike the Alps, glacial processes were limited to a few and reduced areas in the whole central Apennines, and their role can be considered secondary in landscape evolution at a regional scale (e.g. Jaurand, 1999).

The morphotectonic setting of the Abruzzi territory is therefore the result of tectonic cycles and surface processes (apart from glaciation), which have produced different topographic signatures. The schematic geological cross-sections reported in Fig. 4b (see traces in Fig. 3) illustrates the main tectonic units that form the backbone of the mountain belt at shallow crustal levels and their morphological asset. Some DSGSDs crossing the A–A′, B–B′ and C–C′ sections were also reported.

Although masked by the effect of later normal faulting, the Neogene-Early Pleistocene thrust edifice has preserved its topographic wavelength ($\lambda_1$). This is considered as the distance between the culmination zone of NW-SE-oriented mountain ridges derived from the Apennine orogenesis or, similarly, as the distance between leading thrust surfaces. It ranges from 10 to 28 km in southern areas (section A–A′ and B–B′ in Fig. 4b) to about 30 km around the Fucino Basin (section B–B′) and in northern sectors (section C–C′), due to a more intense extensional process. Minor thrusts and back-thrusts mark a shorter, thrust-related, topographic wavelength ($\lambda_2 \leq 5$ km) within the Gran Sasso-Genzana geological domain and partly in the carbonate platform of western Marsica (sections A–A′ and B–B′ in Fig. 4b).

Plio-Quaternary normal faulting originated a similar $\lambda_2 \leq 5$ km topographic signature in the central parts of sections A–A′ and B–B′ and within the Gran Sasso Range in section C–C′. This secondary wavelength characterizes narrow tectonic depressions which are surrounded by elevated mountain ridges and filled by Neogene flysch terrains or Plio-Quaternary continental deposits.

## 3. Methods

The realization of the Abruzzi DSGSDs database followed a multiple-step methodological procedure, including: i) collection of topographic

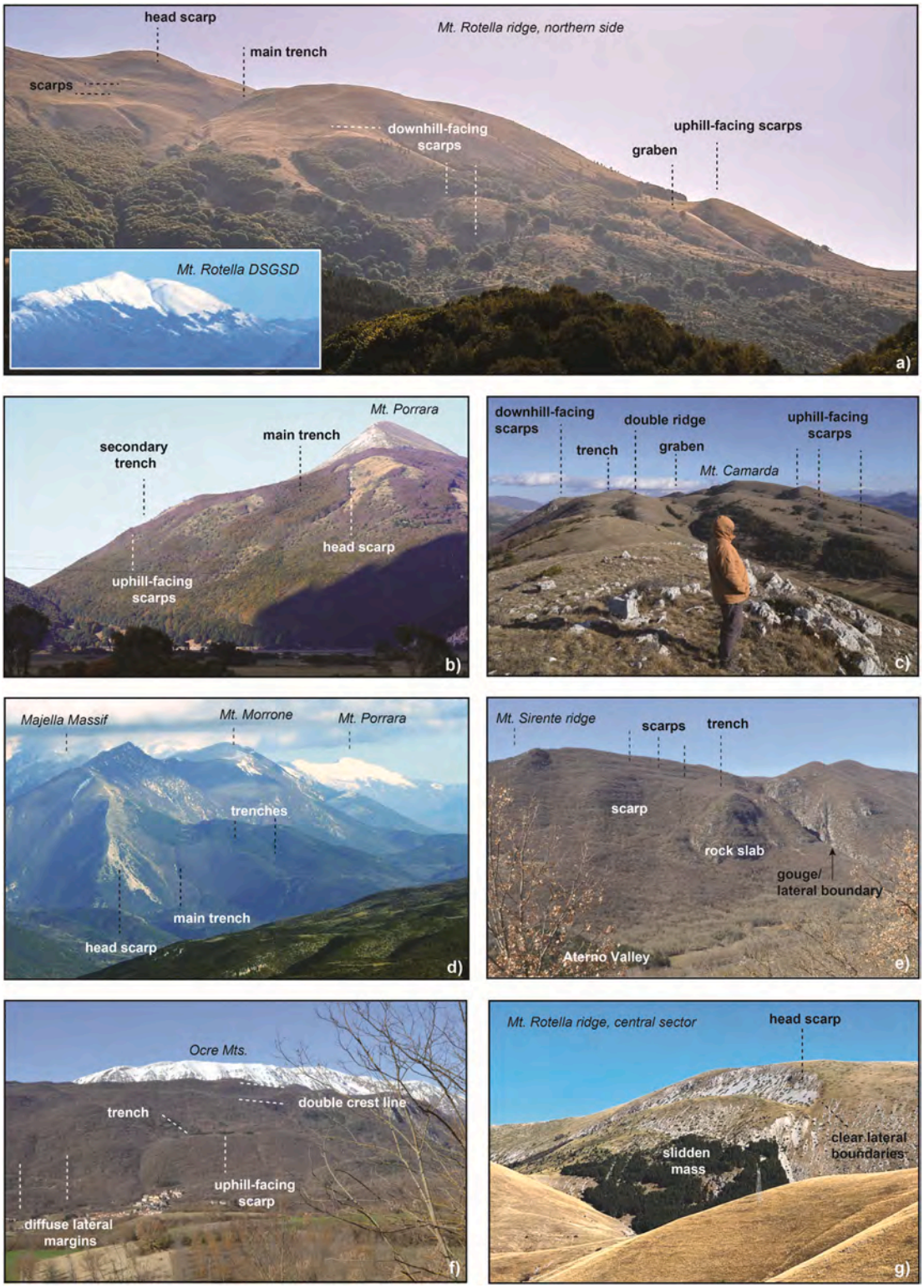


**Fig. 2.** Examples of DSGSDs across the central Apennines: a) Mt. Rotella, north-western edge (panoramic view in the lower left insight); b) Mt. Porrara western slope (Crescenti et al., 1987); c) Mt. Camarda; d) Mt. Morrone, north-western slope (Gori et al., 2014); e) Aterno Valley, Sirente Mt.; f) Stiffe mountain ridge (Khalaf et al., 2025); g) Mt. Rotella western slope, central sector (Galadini, 2006).

raster datasets and aerial photographs series, available from INGV and the Abruzzo Region website (Table 1); ii) implementation of a preliminary GIS database including data from former DSGSDs datasets, as the IFFI (2007) inventory, the CARG database, and other local sources (Table 2); iii) revision of published case-histories documented in the scientific literature and their inclusion in the geodatabase; and iv) insertion of newly-observed DSGSDs.

Most of the 263 (out of 337) new, original DSGSDs cases inventoried were identified through photointerpretation, which is the most effective methodology for DSGSDs investigation at a regional scale, based on the synoptic vision of landscapes (Fig. 5a–d). Different stereoscopes were used (Table 3).

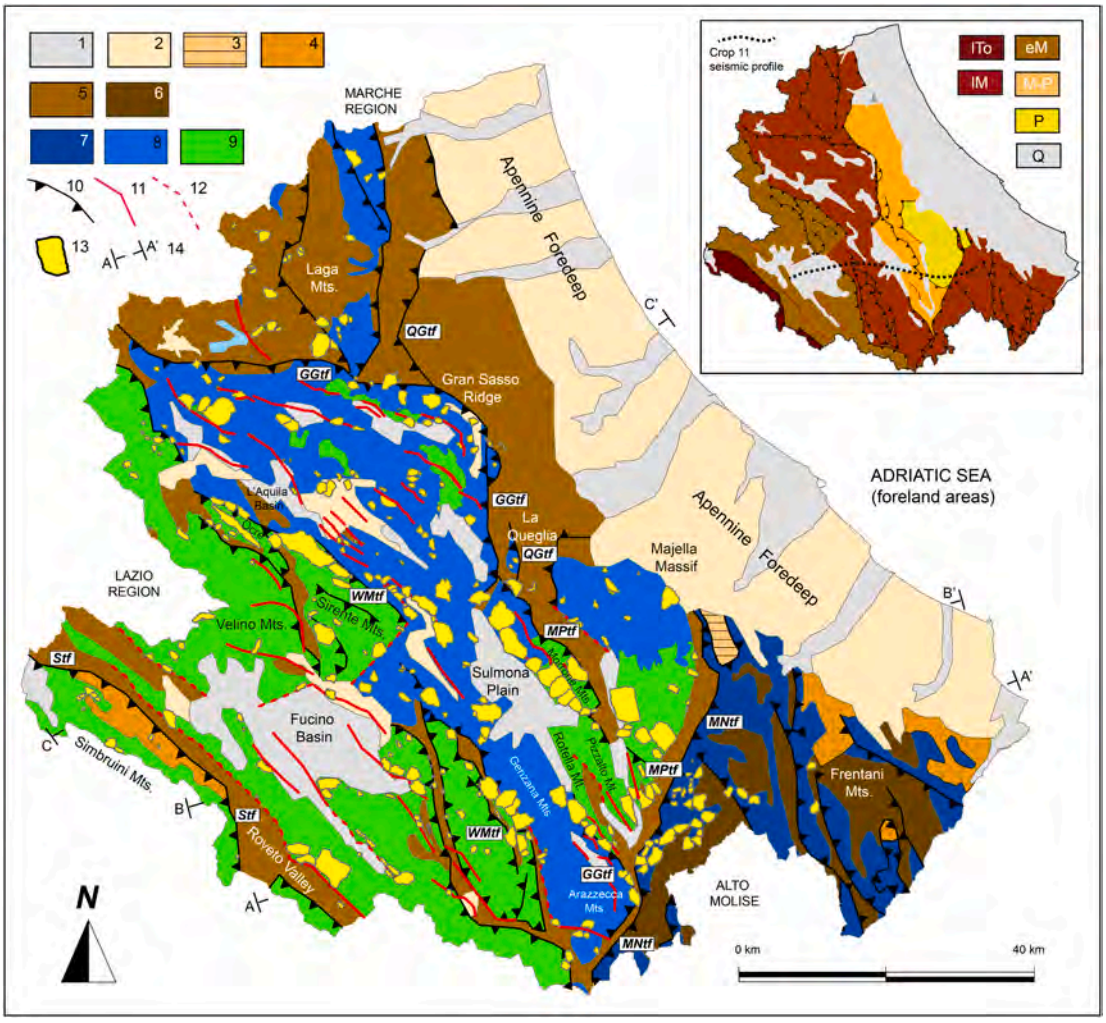


**Fig. 3.** Geological setting of the Abruzzi region (modified after Patacca et al., 1991, 2008). Main geolithological domain (GLD) and tectonic structures are reported. Post-orogenic clastic sequences, foreland and foredeep deposits: 1) Continental and subordinate shore deposits (Holocene-middle Pleistocene); 2) Marine-continental deposits in the peri-Adriatic sector (Lower Pleistocene) and continental deposits in the Apennine intramontane basins (Lower Pleistocene-Pliocene); 3) deformed foreland deposits (Pliocene); 4) Thrust-top deposits (Lowermost Pliocene-Tortonian); 5) Siliciclastic deposits, arenaceous-pelitic, and 6) pelitic-arenaceous (Lowermost Pliocene-Tortonian). Pre-orogenic basin and slope-to-basin sequences: 7) Molise Unit, deep basin and hemipelagic deposits, (Tortonian-Jurassic); 8) Gran Sasso-Genzana, Montagna dei Fiori and La Queglia units, i.e. slope-to-basin (Paleogene-Lower Jurassic) sequences overlain by Miocene open-ramp carbonates. 9) Carbonate platform sequences (Upper Cretaceous-Upper Triassic) and Miocene open-ramp carbonates. 10) Regional thrust front; 11) active normal faults from Galadini and Galli (2000), modified; 12) Plio-Quaternary normal and strike-slip faults from Patacca et al. (2008), modified. 13) DSGSD. 14) Trace of geological cross-sections in Fig. 4b. Legend: GGtf = Gran Sasso-Genzana thrust front; MNtf = Molise nappe thrust front; MPtf = Morrone-Porrara thrust front; QGtf = La Queglia thrust front; Stf = Simbruini thrust front; WMtf = Western Marsica thrust front. Upper right corner: first age of thrust-related deformation and uplift. Legend: lTo = late Tortonian; eM = early Messinian; lM = late Messinian; M-P = late Messinian-early Pliocene; P = early-middle Pliocene; Q = depressed Quaternary sectors. Trace of the CROP 11 crustal profile section as imaged in Fig. 4a is reported.

DSGSD polygons were traced encompassing linear or planar geomorphological features that are considered diagnostic signatures of gravitational deformation when distributed over a slope-to-valley system (Fig. 6): i) ridge doubling extending for lengths in the order of tens to hundreds of meters (Fig. 6a, b); ii) parallel to crosscutting, longitudinal or oblique trenches with metric to decametric length, locally coinciding with shear surfaces (Fig. 6c–g); iii) swarm of straight to curvilinear scarps and counterscarps, also known as downhill and uphill-facing scarps (Fig. 6e, f); iv) valley incisions along lateral edges, often connected to ridge doubling and producing debris fans and scree deposits (Fig. 6g); v) interrupted paleo-landscape features; vi) newly-formed shear surfaces inconsistent with the structural/tectonic inheritance of the mountain ridge; vii) bulging zones and block rotations along the lower sectors of the slope (Fig. 6h); and viii) active erosion areas and secondary landslides along the lateral and basal edges (rockfall, rockslides).

The geomorphological analyses were conducted using passive stereoscopic 3D imaging. A Schneider 3D Pluraview digital stereoscope was preferentially used, having displays with screen diagonals up to 28 in., resolutions up to 4 K (UHD), and a colour depth of 10 bits/pixel. The stereoscopic technique uses images acquired in the same area from two different angles. In our case, this was achieved by utilizing two images acquired during separate transits of the orbiter.

Moreover, the 3D image device uses a semi-reflective mirror to reproduce the stereoscopic effect passively. The two monitors display both images of the stereoscopic pair, with polarization angles differing by 90°. The semi-reflective mirror combines the images, while polarized glasses let each eye view its corresponding image. The glasses achieve this function passively, as they are polarized with a 90° difference, allowing each lens to transmit light from only one of the two monitors. A dedicated free software was developed for stereoscopic visualization (https://zenodo.org/badge/latestdoi/546700017, accessed on 12 April

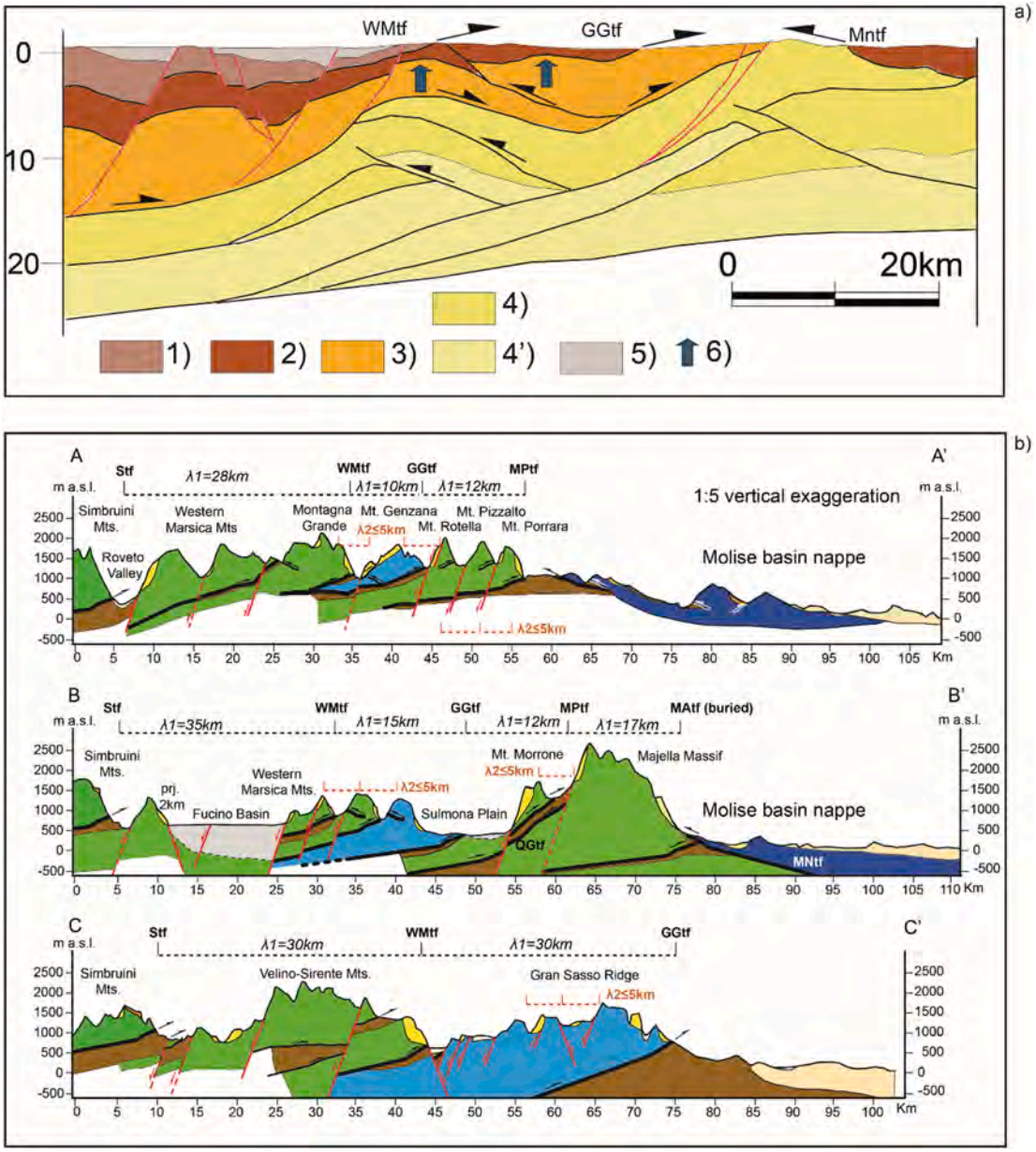


**Fig. 4.** a) Geological cross sections of central Apennines along part of the Crop 11 crustal profile (section in Fig. 3, upper right corner). Portions of the belt are distinguished according to their first involvement in the Apennine structure. Legend: 1) early Messinian; 2) late Messinian; 3) late Messinian-early Pliocene; 4) late-middle Pliocene; 4′) middle-Late Pleistocene (Permo-Triassic stacked section); 5) Quaternary depression; 6) induced, passive uplift due to deep stacking; b) Structural and morphotectonic setting of central Apennines at shallow levels. Traces and legend are reported in Fig. 3.

2025). This stereoscopic technique preserves the full resolution of the original images while enhancing the vertical scale, thus improving the perception of topography and surface features.

Remote sensing analysis was constantly accompanied by field surveys over a five-year period (2020–2024). Only 33 DSGSDs out of 337 were not controlled on field due to logistical impediments. Field checks allowed in some cases a more detailed definition of DSGSD boundaries; however, the maximum error associated with polygon definition through former photoidentification was around 10–15% in terms of areal extension.

Once completed, the dataset was analysed using statistical methods and geospatial techniques. Morphometric characterization of large rock slope deformations was achieved through three key parameters such as: i) DSGSD area; ii) width-to-length ratio (W/L), where width was measured along the slope orientation (parallel to contour lines) and length on the dip direction; iii) height-to-width ratio (H/W), with height determined as the elevation difference between the highest and lowest points in a single DSGSD polygon. The slope geometry instead was delineated by estimates of: iv) mean elevation (i.e. average topography within the portion of slope affected by a DSGSD); v) mean slope gradient; and vi) mean aspect (see Table 4).

Finally, to investigate the relationships between the long-term geological evolution of the belt and spatial distribution of DSGSDs, the Abruzzi region was subdivided into 91 squared sub-areas (10 × 10 km), which were classified according to the age of first involvement in the Apennine belt. Equally sized and arbitrarily located sub-areas average out local controls on DSGSDs distribution, such as slope geometry, lithology, inherited structures, and allow for exploring regional variations (Agliardi et al., 2013).

Apart from DSGSDs density variation, for each squared area, a morphometric analysis of bulk topography was also performed based on a DEM with 10-m resolution (Table 1, Tarquini et al., 2007). Calculated

**Table 1**
Raster dataset used for this work. Legend: GAI = Gruppo Aeronautico Italiano (Italian Aviation Group). AIMA = Azienda di Stato per gli Interventi nel Mondo Agricolo (Public Society for Agricultural Improvement).

| | Type | Code | Scale |
|---|---|---|---|
| Aerial photos | Stereoscopic photographs on analogue support, panchromatic | "GAI" flight 1954 | 1:33,000 |
| | Stereoscopic photographs on analogue support, panchromatic | "Volo Italia" 1988–1989 | 1:70,000 |
| | Stereoscopic photographs on analogue support, b&w | "Volo Italia" 1994, Abruzzi | 1:75,000 |

| | Type/datum | Origin/datum | Scale |
|---|---|---|---|
| Orthophoto | Raster orthophoto, b&w | Digital aerial photography AIMA — Flight 1996, WGS84 | 1:10,000 |
| | Raster orthophoto, panchromatic | Abruzzi Aerial photography Flight 1999–2000, WGS84 | 1:5000 |

| | Type | Origin/datum | Resolution |
|---|---|---|---|
| DEM | DEM, GeoTIFF Format | TINITALY/1.1, WGS84 https://tinitaly.pi.ingv.it/. Tarquini et al., 2007 | 10 m |

| | Type | Origin/datum | Scale |
|---|---|---|---|
| Topography | Raster topographic map | Abruzzi Topographic Map, 1995 edition, WGS84 | 1:25,000 |
| | Raster orthophoto maps, WGS84 | Abruzzi Topographic Map, 1987 aerial survey, WGS84 | 1:10,000 |

**Table 2**
Former datasets used for this work.

| Databases | Type | Origin/datum | Scale |
|---|---|---|---|
| DSGSDs database | Vector database/ polygon | Italian Geological Map (CARG), sheet 348–349, 358–360, 367–369,378 | 1:50,000 |
| DSGSDs database | Vector database/ polygon | Italian Landslide Inventory (IFFI, 2007) | 1:50,000 |
| Landslide databases | Raster database/ polygon | Abruzzi hydrographic basins landslide map. | 1:25,000 |
| Landslide databases | Raster database/ polygon | River Basin Authority (Liri-Garigliano and Volturno rivers) hazard map | 1:25,000 |

parameters included: $H_{min}$, that is the minimum elevation representing the local base level; $H_{max} - H_{min}$, corresponding to the local relief, which reflects interactions between tectonics and erosional processes; $H_{mean} - H_{min}$, or average altimetric range, used as an index of valley incision down to the local base level (with high values representing large elevated areas with a few deeply incised streams); the standard deviation of slope ($\sigma_s$), expression of slope roughness.

Finally, the standard slope gradient for slopes hosting a DSGSD was calculated both within the area under gravity-driven deformations and outside for a buffer distance of 2 km. Results are thought to indicate the impact of DSGSD on the evolution of local topography.

## 4. Results

### 4.1. DSGSDs inventory and statistical analyses

The DSGSDs inventory covers a territory of 10,763 $km^2$, or 6996 $km^2$ if only mountain areas with elevations higher than 600 m a.s.l. are considered. It includes 337 sites documented from different sources (Fig. 7). After a careful revision, some records from IFFI (Italian Landslides Inventory, 31 sites), CARG (Regional Geological Map of Italy, 10 sites), or both databases (5 sites) were preserved. Original DSGSDs from this work are 291, 263 previously unknown, and 28 reinterpreted from the scientific literature.

In this section, results of statistical analyses on the DSGSDs database are presented. Variability of geometric parameters for the 337 documented case-histories – Area, H/L and W/L ratios – are reported in Fig. 8a–c. Morphological variables of the hosting ridges – mean values of slope elevation, aspect, and gradient – are illustrated in Fig. 8d–f. Table 4 reassumes the main values.

The DSGSDs frequency-area distribution shows that portions of slope areas involved in gravitational deformation are mainly between 0.50 and 2.00 $km^2$ (Fig. 8a). More precisely, Table 4 reports a mean value of 1.68 $km^2$, and 25th and 75th percentile values equal to 0.44 $km^2$ and 1.84 $km^2$, respectively. Nevertheless, Fig. 8a evidence several outliers (n = 31, <5th and >95th percentiles) filling a DSGSDs subsample with large areas, between 4.00 and 8.00 $km^2$. Actually, six DSGSDs affect mountain areas even larger than 10.00 $km^2$. Regarding the width/length ratio (W/L), values are generally >1.00, indicating that DSGSDs are usually elongated along the slope direction (Fig. 7b and Table 4). The height/length ratio (H/L) has a reduced statistical dispersion (Fig. 7c), with mean and median values around 0.40 (Table 4). Moreover, values are basically <0.50 (75th percentile equal to 0.47), thus implying DSGSDs have preferentially an internal elevation difference half their length.

The slope geomorphological variables also gave some indications. Between the 25th and 75th percentiles the distribution of the slope mean elevation (average topography) ranges between 0.89 and 1.33 km (Table 4 and Fig. 8d). Regarding the slope gradient, unimodal distribution evidence a 22° mean value (Fig. 8e). Finally, the aspect is reduced to two preferential orientations, with slopes interested by DSGSDs facing towards NE or S-SW (Fig. 8f).

As the final statistical analysis of the DSGSDs database, Fig. 9 presents a logarithmically binned, non-cumulative frequency-density distribution of rock slope deformation areas. The frequency density, defined as f = dN/dA, is plotted as a function of the planar area A. Here, dN represents the number of DSGSDs whose areas fall within the interval [A, A + dA], where dA is the width of the area bin. Logarithmic binning is adopted to ensure adequate sampling over several orders of magnitude in DSGSD size and to reduce statistical noise in large areas. For DSGSD larger than a certain area, i.e., the rollover area in Fig. 9, the size-frequency distribution can be interpolated with a power-law function:

$$f(A) = aA^{-b} \quad (1)$$

Both the rollover and the scaling coefficients "a" and "b", equal to 1.01 $km^2$, 1.70e+02, and 2.08, are determined by best fitting the data in Fig. 9.

A subset of 159 out of 337 DSGSDs (47%) is characterized by A > 1.01 $km^2$. Deflection from the power-law behaviour occurs below the 1.01 $km^2$ threshold and concerns the remaining 178 DSGSDs.

### 4.2. Influence of regional geology

Once the standalone geometric parameters were analysed, the potential influence of geological conditions on the DSGSDs regional distribution and size was investigated, considering the prevalent lithology encompassed by each polygon (see Fig. 3).

In the geolithological domain of carbonate platform sequences (CPL in Fig. 10), limestone and dolomites prevail in the Mesozoic sections, whereas biodetritic limestone, marly limestone, and subordinate marls characterize the Neogene, open ramp sequences. Prevalent lithologies in the slope-to-basin sequence (SLB) include Meso-Cenozoic resedimented biodetritic limestone and breccias interlayered with marly limestone, marls, and cherty limestone. Miocene foredeep deposits (FOR),

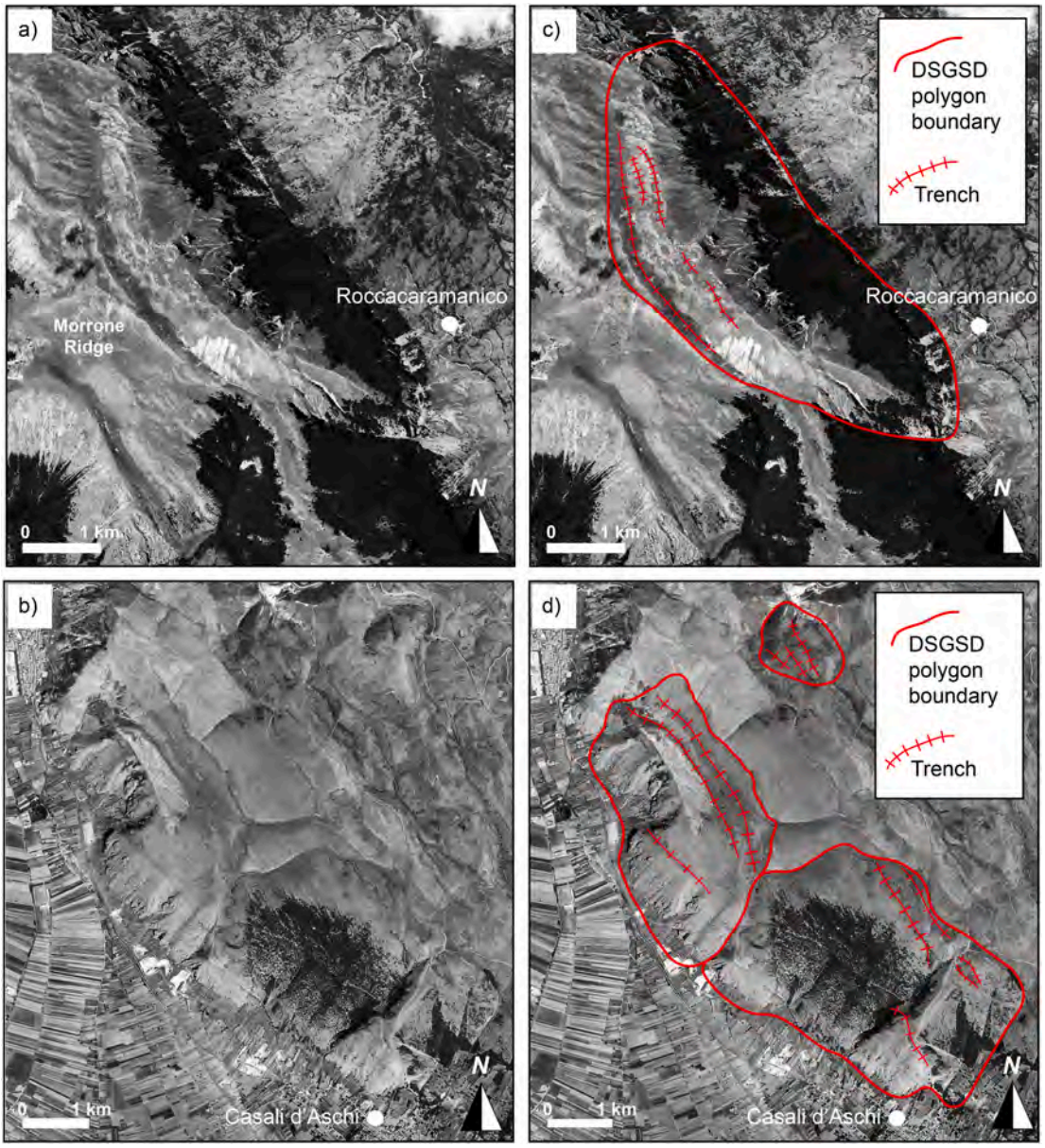


**Fig. 5.** a) Aerial photos from *Volo Italia 1944*: a) stripe 51b, frame 8018 (Mt. Morrone eastern slopes), and b) Strip n. 52b, frame 6096 (eastern border of the Fucino Basin), with examples of photointerpretation reported in c) and d), respectively.

**Table 3**
Instruments setting. Legend: UHD = ultra high definition.

| Instrument | Equipment/use | Magnification |
|---|---|---|
| Aviopret Wild APT-1 stereoscope | Variable focal length optical system | 3–15.5× |
| TOPCON MS-3 Wild ST4 mirror stereoscope | Observation at different frame scales allowed | 3–8× |
| Schneider 3D Pluraview digital stereoscope (Used for the high-altitude "Volo Italia") | Wide view angle, up to 4 K (UHD) with 8.3 megapixels per eye and 10-bit colour depth. | Maximum resolution allowed |
| Sokkia pocket stereoscope | Field survey support | 2.5× |

overlying both CPL and SLB sequences, are made up of sandstones and subordinate claystones. A large fraction of clays features the Upper Cretaceous-Oligocene sequence of the Molise geological sequence (BASm), overlayed by a section of Miocene biodetritic and cherty carbonates and marls passing upwards to clayey flysch deposits (FORm). Finally, Plio-Quaternary thrust top basin (TTB) and post-orogenic (POR) deposits are mainly composed of reworked, carbonate clastic materials.

The frequency distribution histograms in Fig. 10a report the number of DSGSDs documented within each Apennine geolithological domain (GLD) as represented in Fig. 3. An almost equal number of case histories were documented for the slope-to-basin sequences of the Gran Sasso-Genzana-La Queglia units (128) and the Carbonate Platform sequences (115). Considering their comparable regional extension (1853 and 2021 $km^2$, respectively), the ratio between the DSGSDs cumulative area and the total extension of the GLDs results in a similar value (Fig. 10b). A main difference between the two GLD concerns the DSGSDs dimension. The mean DSGSDs area is almost a third lower for the slope-to-basin sequence (Fig. 10c), while the much higher standard deviation for DSGSDs in the carbonate platform sequence (Fig. 10d) suggests wide data dispersion, likely due to very large phenomena (outliers), as it will be further discussed.

Despite their considerable extent (2139 $km^2$), foredeep deposits of the central and northern sectors of the Abruzzi region host only 56

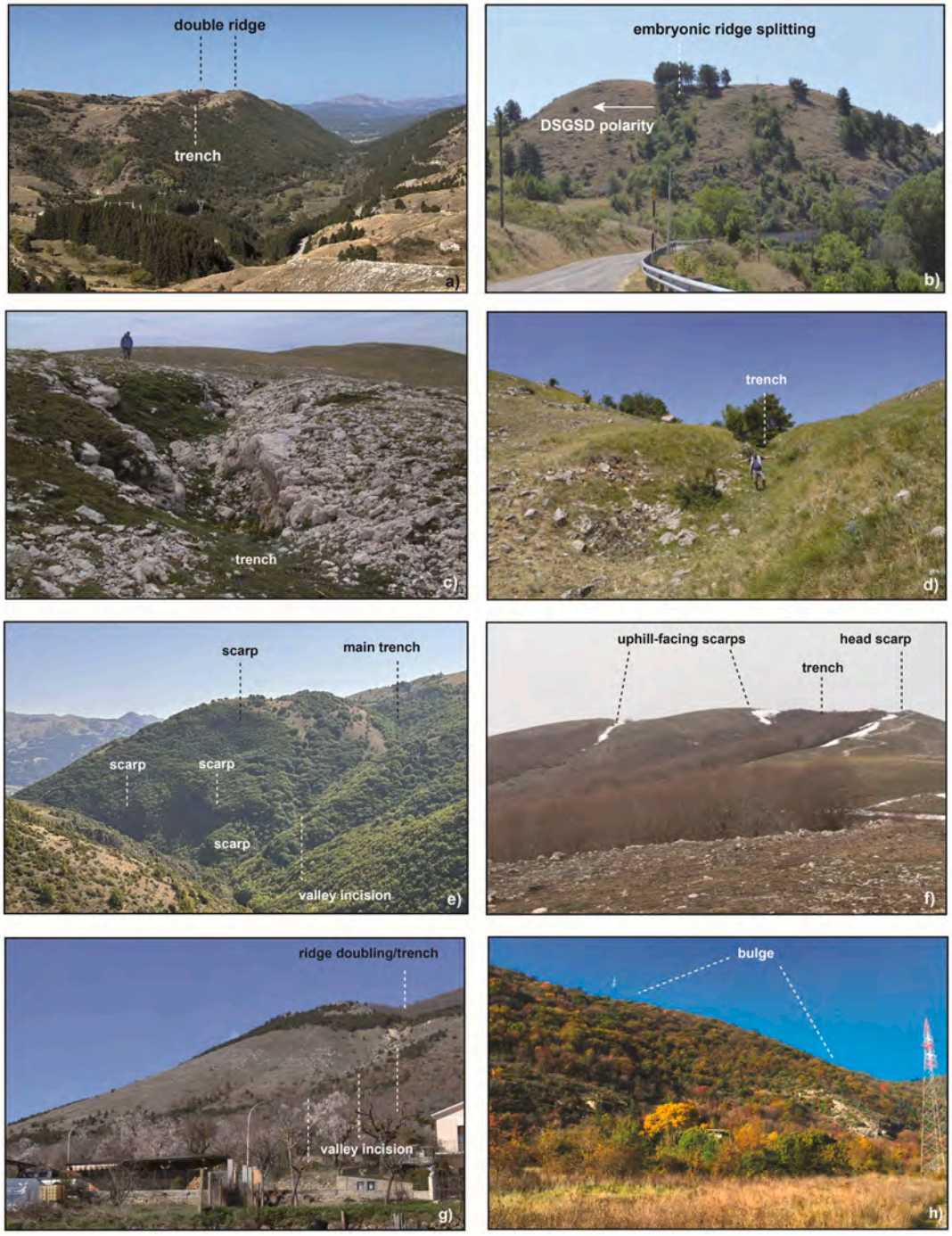


**Fig. 6.** Geomorphological evidence of DSGSDs: a) mature and b) embryonic double ridge on top slope areas; c; d) main trenches, plurimetric in length and width; f) secondary scarps affecting a deforming rock mass separated from the stable ridge by a main trench behind; g) swarm of uphill-facing scarps or counterscarps; h) main valley incision marking the lateral boundary of a DSGSD and connected to ridge doubling at the top of the slope; i) bulge morphology along a slope to valley transition zone.

**Table 4**
Statistical results for the DSGSDs morphometric parameters and slopes morphological variables (reported in italics).

| | Mean | Median | Std dev | Min | Max | 25th %tile | 50th %tile | 75th %tile |
|---|---|---|---|---|---|---|---|---|
| Area (km$^2$) | 1.68 | 0.86 | 2.42 | 0.05 | 20.17 | 0.44 | 0.86 | 1.84 |
| Width/length | 1.38 | 1.35 | 0.60 | 0.32 | 3.78 | 0.96 | 1.35 | 1.72 |
| Height/length | 0.39 | 0.36 | 0.19 | 0.07 | 1.37 | 0.27 | 0.36 | 0.47 |
| *Mean elevation (km)* | *1.13* | *1.12* | *0.34* | *0.32* | *2.19* | *0.89* | *1.12* | *1.33* |
| *Mean slope gradient (°)* | *22.37* | *21.62* | *5.59* | *7.23* | *41.50* | *18.83* | *21.62* | *25.37* |
| *Mean aspect (°)* | *165.94* | *190.97* | *94.68* | *2.97* | *359.89* | *71.94* | *190.97* | *238.10* |

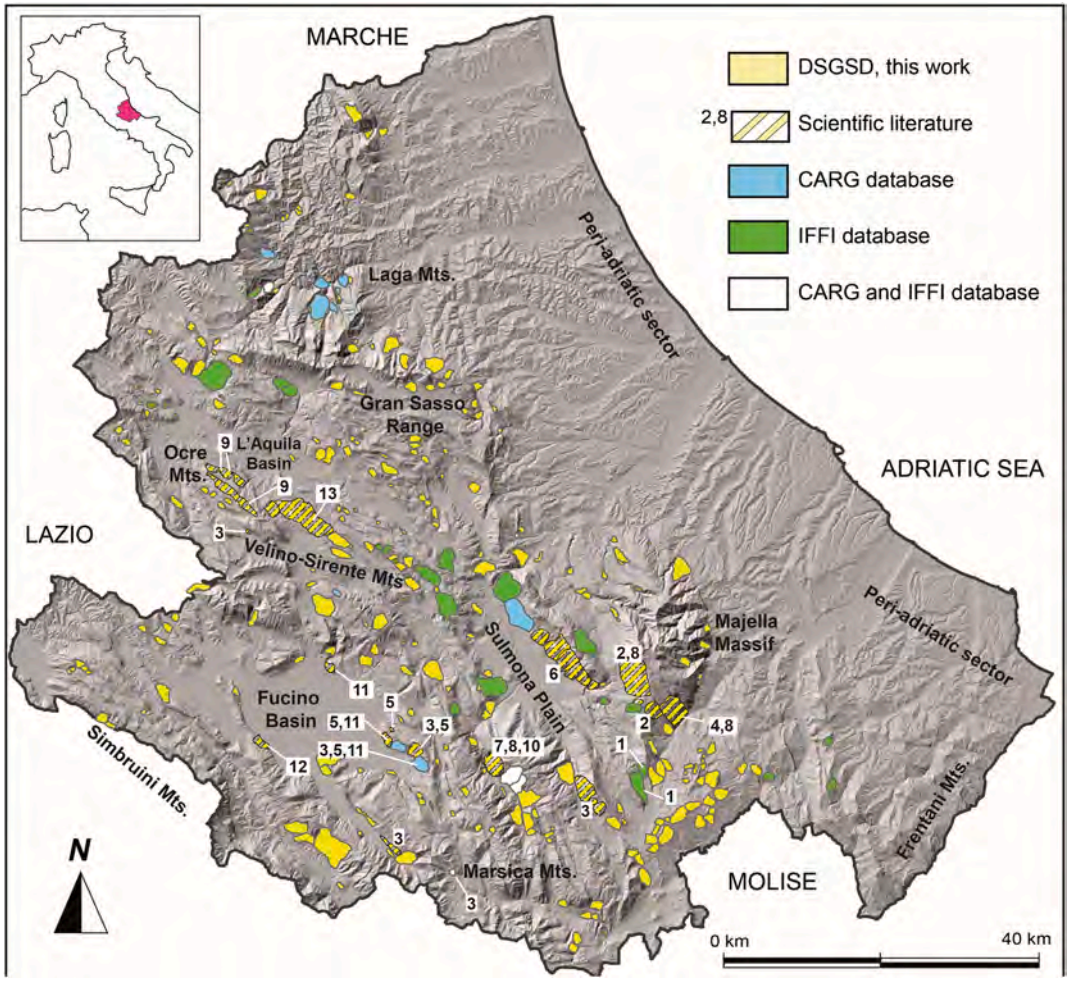


**Fig. 7.** DSGSDs inventory for the Abruzzi region after this work, including 337 sites (hillshade map is derived from SRTM30m topographic dataset). Legend: 1) Crescenti et al., 1987; 2) Di Luzio et al., 2004a; 3) Galadini, 2006; 4) Scarascia Mugnozza et al., 2006; 5) Moro et al., 2012; 6) Gori et al., 2014; 7) Esposito et al., 2013; 8) Bianchi Fasani et al., 2014; 9) Albano et al., 2015; 10) Della Seta et al., 2017; 11) Del Rio et al., 2021; 12) Di Luzio et al., 2022 and Discenza et al., 2023a; 13) Khalaf et al., 2025.

DSGSDs (Fig. 9a), with a reduced total area under gravitational deformation (Fig. 10b). Also, the mean areal extension is low (1.07 $km^2$) for DSGSDs developed in arenaceous turbiditic sequences (Fig. 10c).

A non-negligible number of DSGSDs were found within the Molise (deep) basin sequence, but again, only a few in the related foredeep deposits (23 and 7 in Fig. 10a, respectively). Interestingly, the first group is characterized by the third value (0.04) of the cumulative DSGSDs area/GLD extension ratio (Fig. 10b).

Finally, a few case histories were documented in the post-orogenic clastic deposits (5, mainly around the Fucino Basin) and the thrust top deposits (2). The first group has a considerable mean area (1.69 in Fig. 10c), demonstrating that DSGSDs of non-negligible size can originate in Plio-Pleistocene, continental, clastic deposits.

### 4.3. Relationships with main tectonic features

A geospatial analysis was performed using a buffer technique to identify DSGSD areas surrounding the main Apennine tectonic features. A 1 km-wide buffer zone was created along thrust fronts (Patacca et al., 1991, 2008) and Plio-Quaternary faults (Galadini and Galli, 2000; Patacca et al., 2008) shown in Fig. 3. Linear clusters were identified in both cases (Fig. 11a, b). Where normal faults run near thrust traces, DSGSD can be present in both datasets (34 cases).

Overall, 142 DSGSDs out of 337 (42%) are found along a 1 km distance from a thrust front in the Abruzzi territory. From SE to NW, the proximity of DSGSDs to thrusts is evident along: i) the MNtf and internal thrusts of the Molise nappe, i.e. MNit (Fig. 11a and sections A–A′ and B–B′ in Fig. 4); ii) the MPtf, (Fig. 11a and sections A-A'); iii) the GGtf (Fig. 11a and sections B–B′ and C–C′), on the edges of the Arazzecca and Genzana Mts. and the Gran Sasso Ridge in particular; iv) the Montagna Grande and Sirente main and secondary thrusts, being part of the Western Marsica thrust system (i.e. WMtf in Fig. 11a and sections A–A′ and B–B′); the QGtf and secondary thrusts within the Laga siliciclastic domain (Fig. 11a).

Analogously, a subset of 165 DSGSDs (49%) concentrate along the trace of main Plio-Quaternary normal and strike-slip faults (Fig. 11b). Main clusters are identified: i) on the SW slopes of the Majella Massif (Fig. 11b and section B–B′); ii) along the southwestern edge of the Morrone-Porrara ridge (Fig. 11b and sections A–A′ and B–B′); iii) along the western border of the Genzana Mts. (Fig. 11b and section A–A′); iv) on the sides of the narrow, NW-SE-oriented valleys at the south-eastern edge of the Fucino Basin (Villavallelonga, Giovenco valleys) (Fig. 11b); v) along the wide Roveto and Aterno valleys located in the south-western and central sectors of the region, respectively (Fig. 11b); vi) within the north-western sector of the Gran Sasso Range.

### 4.4. DSGSDs distribution and long-term tectonic history of the belt

The base map reporting the first age of thrusting experienced during the Mio-Pliocene orogenesis was divided through a 10 km wide fishnet

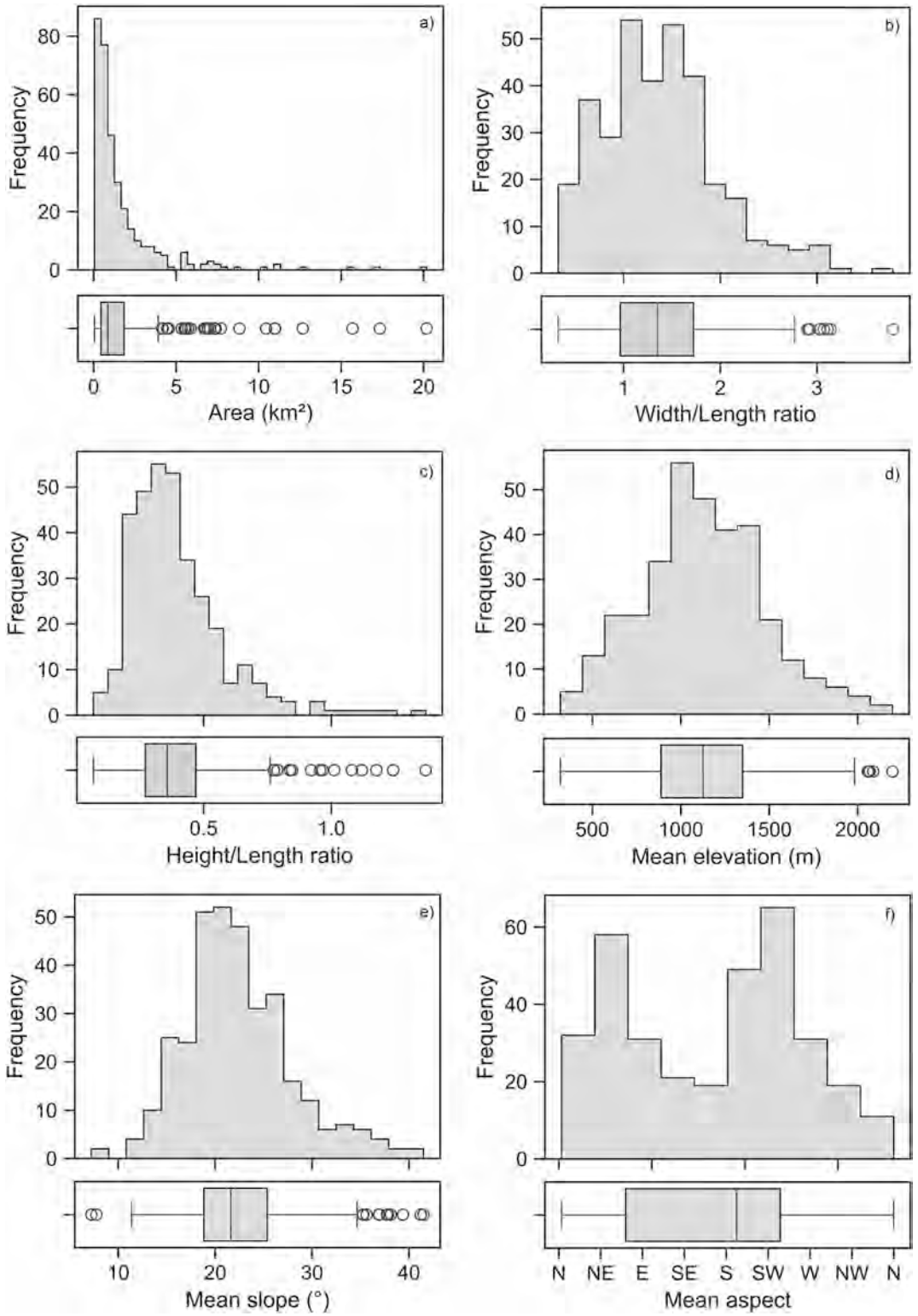


**Fig. 8.** Frequency histograms and boxplots derived from the DSGSDs morphometric parameters (a–c) and slope morphological variables (d–f). Central marks in boxes below graphs indicate the median, while the lateral edges indicate the 25th and 75th percentiles, respectively. Extreme data, with limits corresponding to the 5th and 95th percentiles, are represented by whiskers, whereas outliers (<5th and >95th percentiles) are plotted individually as a circle.

(Fig. 12a), and the DSGSDs density calculated (Fig. 12b). Density values, which are expressed as the ratio between the total area involved in slope deformations within a square cell and the cell dimension, range from 0.30 to 0.02. Linear clustering along thrust fronts and active normal faults still prevails and explains the high-density areas (0.30–0.19) in the central and southern sectors of the region, with an apparent E-W trend. However, without considering linear clustering, it was found that large rock slope deformations concentrate within the late Messinian sections of the belt and, subordinately, along the eastern edge of the early Messinian sector. Indeed, a continuous zone with a NW-SE orientation and density values between 0.19 and 0.10 can be observed in the central sector of the study area (Fig. 12b), roughly corresponding to the

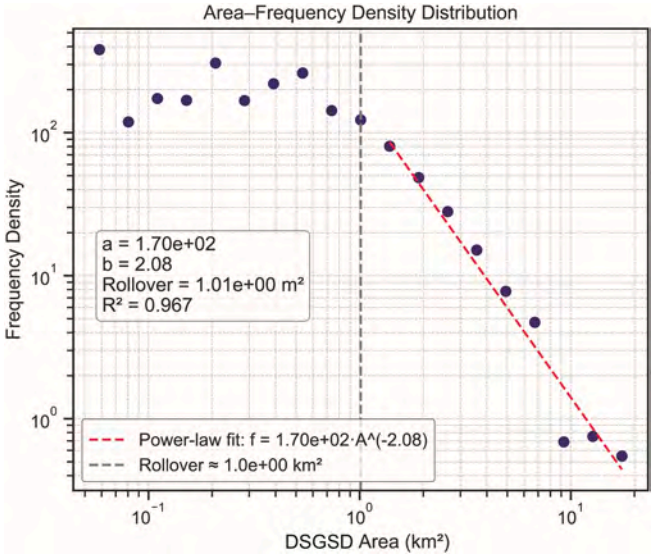


**Fig. 9.** Log–log plot of the DSGSDs size-frequency density distribution in the regional inventory. Each point represents a bin of the logarithmically spaced area classes, where the frequency density is computed as the number of DSGSD within each bin divided by its width. The dashed red line indicates the best-fitting power-law relationship, while the vertical grey line marks the roll-over area.

southern sector of the Genzana-Gran Sasso domain (see Fig. 3). Therefore, the SW-NE tectonic polarity of the orogen can be disregarded as a factor controlling DSGSD distribution, which does not depend on the age of first deformation and rock damage. However, it can be noted how the late Messinian portion of the belt is found above stacked units at mid-crustal levels (Fig. 4c). As it will be further discussed, the deep structural architecture and the long-term tectonic evolution of the Apennine belt (Patacca et al., 2008) can give an alternative explanation for DSGSD density distribution.

### 4.5. Bulk topography and DSGSDs distribution

DSGSDs density shows a positive correlation with the local relief $H_{max} - H_{min}$ calculated for the 91 squared areas and for all subsets of data (Fig. 13a). For DSGSD included in the late Messinian portion of the belt, a linear regression function was estimated:

$$y = 1.14e^{-4}x + 8.44e^{-4} \quad (2)$$

Similarly, a positive correlation is established (Fig. 13b) with the average altimetric range $H_{mean} - H_{min}$; again, the behaviour of the late Messinian data can be expressed with a linear regression function:

$$y = 6.5e^{-5}x - 00157 \quad (3)$$

On the contrary, negative correlation is evident between DSGSDs density and the slope roughness (Fig. 13c). Indeed, DSGSDs higher values were found for a moderate standard deviation of the slope gradient (10°–12°), while low density values were estimated for low (<10°) and high (>12°) standard deviation values (Fig. 13c).

Favourable conditions for the onset and development of DSGSDs in the Abruzzi territory are, therefore, an elevated local relief and average altimetric range, whereas slope roughness must show moderate values. This agrees with evidence from Agliardi et al. (2013) who found similar correlations. Focusing on the late Messinian sector of the belt, where a DSGSDs concentration out of linear clustering was observed (Figs. 12a, b), it can be noted how this subset shows higher density than others subset for higher values of both local relief (Fig. 13a) and average altimetric range (Fig. 13b), and lower values of slope roughness (Fig. 13c).

### 4.6. DSGSD impact on local topography

Morphological features associated with a DSGSD are thought to leave a signature on slope topography. Fig. 13d shows the relative frequency distributions of slope angle, estimated from all the values computed from the DEM inside mapped DSGSDs areas and in the neighbouring regions within 2-km buffers, both fitted with a lognormal distribution curve. The buffer distance of 2 km was chosen to investigate areas with similar lithology and marked by the same tectonic features with a morphogenetic role. Unlike evidence from the European Alps (Agliardi et al., 2013), the lognormal fits indicate that slope roughness shows higher values within DSGSDs than outside areas under gravitational deformation.

A DSGSD can modify slope topography also when secondary landslides occur along its edges. However, comparison between the national dataset of landslides (IFFI, 2007) and the DSGSDs inventory presented in this paper showed that only 9.13% of landslide areas are included in DSGSDs polygons.

## 5. Discussions

Results of this work implied a new awareness about the role played by DSGSDs as a landscaping factor in the Quaternary morphogenesis of the central Apennines. The total area covered by the 337 DSGSDs is 573.6 km$^2$, which corresponds to 5.3% of the regional territory (10,763 km$^2$). Nevertheless, if only the 6996 km$^2$ of Abruzzi mountainous territory is considered (i.e. areas with elevation higher than 600 m a.s.l.), the same percentage rises to 8.2%. By comparison, the total extent of Rock Slope Failures, including rock slope deformations comparable to Apennine DSGSDs, is 0.6% of mountain areas in the British highlands (Jarman and Harrison, 2019), 5% in the Alps territory (Agliardi et al., 2012, 2013) and 2% in the New Zealand Southern Alps (Allen et al., 2011).

Oversampling of small DSGSDs in the presented database may be the cause of the large area percentage. This hypothesis could be supported by evidence from the frequency-density distribution of DSGSDs area shown in Fig. 9. Indeed, a power-law behaviour indicates a strict relationship between the frequency and the size/magnitude of a geological process. Consequently, only the 156 features with an area greater than 1.01 km$^2$ might be identified as "pure" DSGSD. The random distribution below the threshold value could still refer to DSGSD whose dimensions may depend on local geological, climatic, and anthropogenic factors. However, adopting this approach, the total DSGSDs area would slightly decrease to 488.60 km$^2$, resulting in a similar 7% percentage.

Alternatively, two main explanations can be found to understand the reason for the considerable extension of large-scale rock slope deformation in the Abruzzi region with respect to other mountain territories.

The first is the number of outliers (31) showing areas >4 km$^2$ (Fig. 8a), whose location is reported in Fig. 14. These exceptionally large phenomena contribute to an overall extension of 242.0 km$^2$, which is 49.5% of the total DSGSDs area (488.60 km$^2$). The second one concerns glacial processes, whose limited action in landscape modelling of the Apennine region during the Quaternary has preserved DSGSDs morphological features from severe erosion, leaving large areas undisturbed. Not by chance, these large DSGSDs (A > 4 km$^2$) are absent in the most elevated, core zones of the Gran Sasso Ridge, Majella Massif, and Velino Mts., where the ice-cover and related erosion processes concentrated during the last Wurm glacial period (Jaurand, 1999).

Still focusing on the DSGSDs population with A > 4 km$^2$, three groups can be identified on the map reported in Fig. 14:

1. DSGSDs found within the forelimbs of main thrust-related structures, such as the Majella, Morrone-Porrara, Sirente, Genzana, and Gran Sasso (see also Fig. 4b, profiles B–B′ and C–C′). These huge DSGSDs gather along E to NE-dipping slopes of mountain ridges corresponding to the main regional thrust fronts and thereby defining the

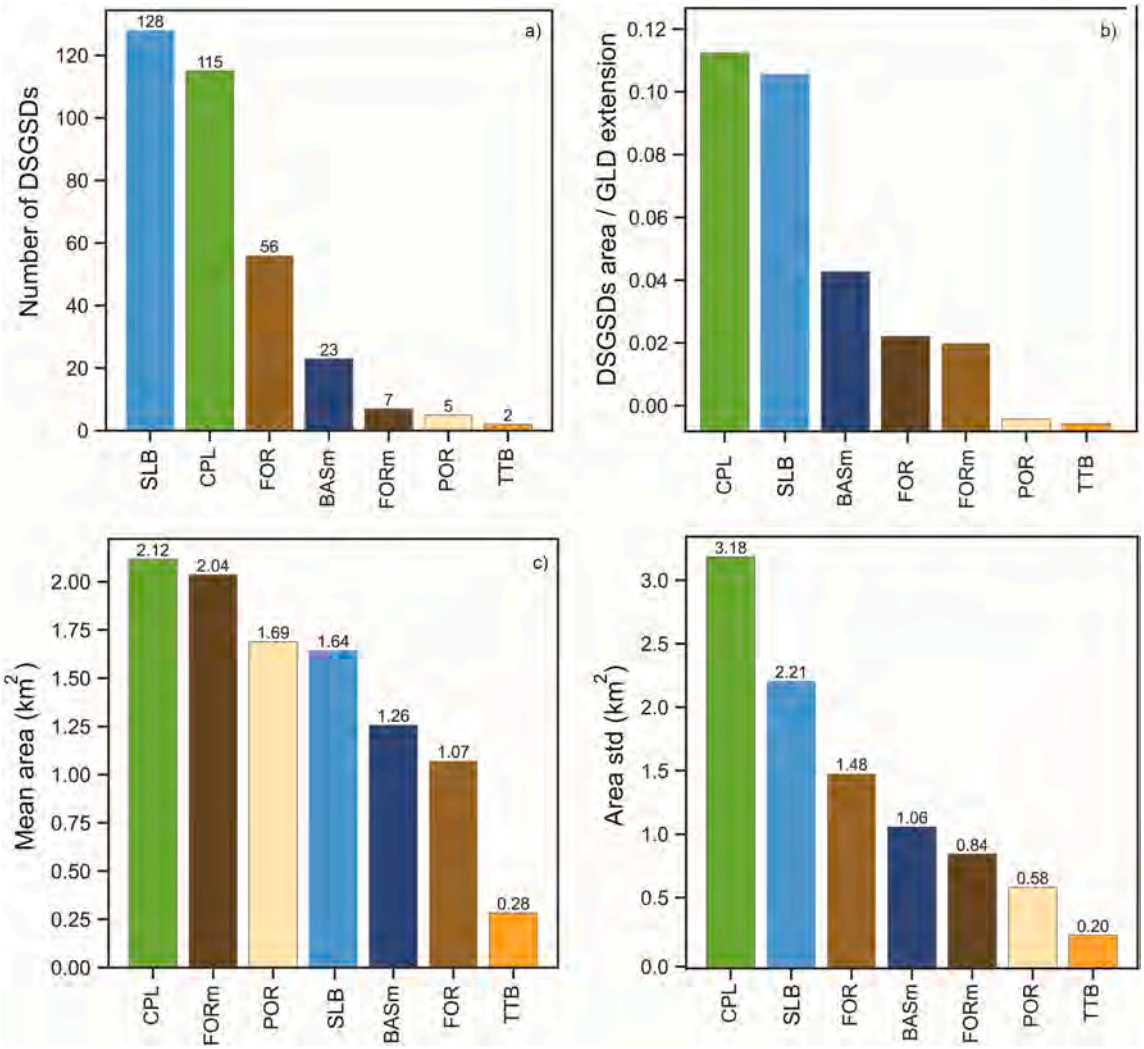


**Fig. 10.** a) Number of DSGSD cases versus Apennine geolithological domain (GLD); b) cumulative DSGSDs area/GLD extension ratio; c) mean and d) standard deviation values of DSGSDs areas for each GLD. Legend: BASm = BASin deposits (Molise geological sequence); SLB = Slope-to-Basin sequences (Gran Sasso-Genzana-La Queglia domain); CPL = Carbonate Platforms sequences (Marsica and Apulia platforms undistinguished); FOR = FOREdeep deposits (central-northern sectors of the Abruzzi region); FORm = FOREdeep deposits belonging to the Molise geological sequence; POR = Post Orogenic clastic deposits; TTB = Thrust Top Basin deposits.

λ1 topographic wavelength of the orogenic belt. Among them, the Stiffe DSGSD (Khalaf et al., 2025) is the largest case identified in the central Apennine, with an area under deformation of about 20 km$^2$. For these cases, sliding and spreading processes are the main mechanisms, with a non-negligible amount of horizontal displacement for involved rock masses;

2. DSGSDs nesting along backlimb zones structures developed mainly in the Apulian carbonate domain (i.e. Majella, Morrone, Porrara, Rotella structures) and secondarily in the Gran Sasso-Genzana domain (see also profiles A–A′ and C–C′ in Fig. 4b). This group contains several DSGSDs extending for more than 10 km$^2$ along the SW slopes of mountain ridges, and ascribable to sackung type of mechanism with vertical movements prevailing. Patacca et al. (2008) and Bianchi Fasani et al. (2014) interpreted these ridge-scale deformations as evidence of backlimb gravitational collapses, which, in turn, developed to accommodate deep staking and passive uplift of buried antiformal structures;
3. DSGSDs localized along intramontane valleys bounded by Plio-Quaternary faults and featuring the $\lambda_2$ topographic wavelength (see Fig. 4b, all sections), or even far from any tectonic lineaments (Fig. 14).

Beyond considerations on the areal extent and size of huge gravitational deformation, the results of this work have evidenced two dominant linear clusters for DSGSDs in the Abruzzi region (Fig. 11a, b).

A first cluster concerns the traces of NW-SE-oriented, NE-verging thrusts (Fig. 11a). In the central Apennines, this kind of tectonic boundary is often characterized by the rheological contrasts among stiff calcareous rocks in the hanging-wall sectors and flysch deposits in the foot-wall zones, these last composed of more deformable arenaceous/clayey rocks. Large spreading or sliding processes can affect the mountain front (Fig. 5a–c). A further cluster is evident along the traces of Plio-Quaternary normal and strike-slip faults (Figs. 11b and 5b–d). The role of active tectonics in driving DSGSDs processes was already discussed by Galadini (2006).

Local lithology is another key aspect conditioning DSGSDs distribution and size. The number of observed cases is similar for the main GLDs of the Abruzzi territory, i.e. the carbonate platform and the slope-to-basin domains (128 and 115 cases, see Fig. 10a).

However, DSGSDs within the neritic, shallow marine sequence have a greater mean area (2.12 vs 1.64 km$^2$ in Fig. 10c), while the larger standard deviation (Fig. 10d) accounts for several outliers (A > 4 km$^2$). This evidence may be explained considering: i) the presence of persistent

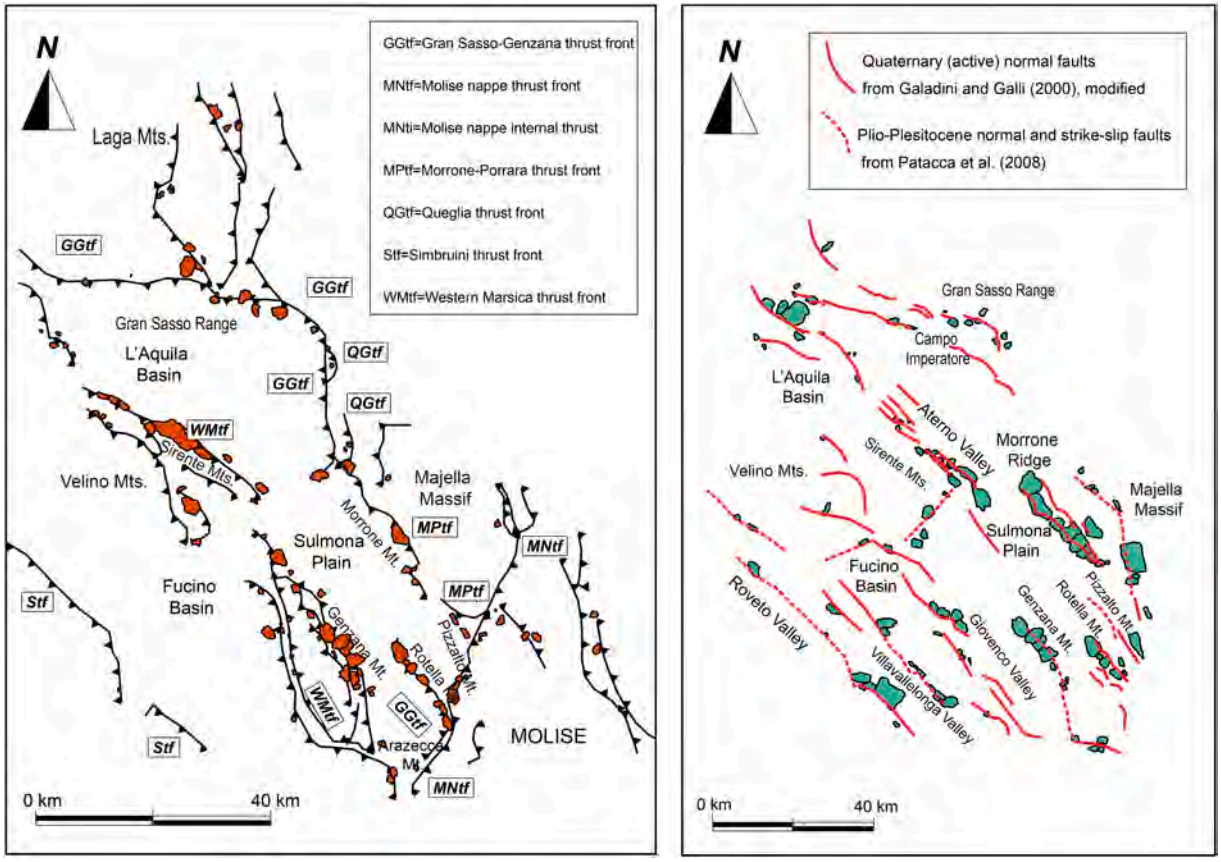


**Fig. 11.** a) DSGSDs linear clustering along main thrust fronts (legend in Fig. 3) in central Apennines after the buffer analysis (1 km); b) results of the same analysis along Plio-Quaternary normal and strike-slip faults.

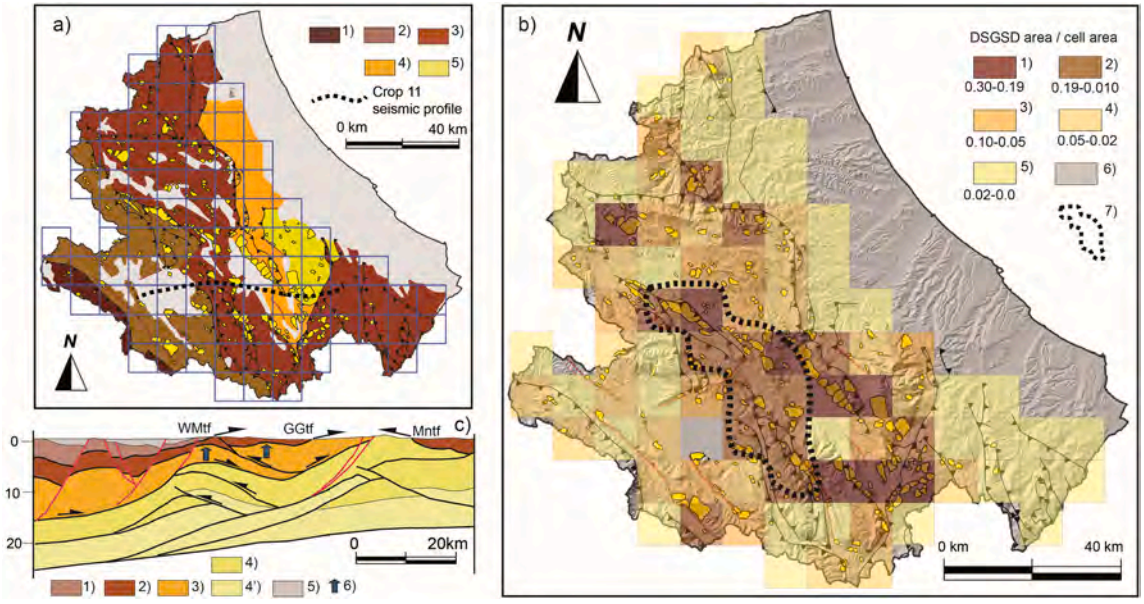


**Fig. 12.** a) Zonation of the Abruzzi territory depending on the age of thrusting and the 10 km wide fishnet. Legend: 1) late Tortonian thrusting; 2) early Messinian; 3) late Messinian; 4) late Messinian-early Pliocene; 5) early-middle Pliocene; b) density map: values are reported in boxes 1)–5); 6) Quaternary depressed areas with no DSGSDs; 7) boundary of high-density extended zone in the central sector of the belt; c) Crop 11 profile, see Fig. 4a for legend.

(hundreds of meters long) brittle deformation features in carbonate rocks isolating large volumes, then utilized by a DSGSD, or ii) the role of thin bedding in calcareous-marly-cherty multilayers of the slope-to-basin domain, acting as localized mechanical discontinuities and driving smaller sliding phenomena.

Large-scale rock slope deformations are rare in foredeep deposits of the central and northern sectors of the Abruzzi region (Fig. 10a, b). This occurs because flysch terrains lie at the bottom of narrow valleys and

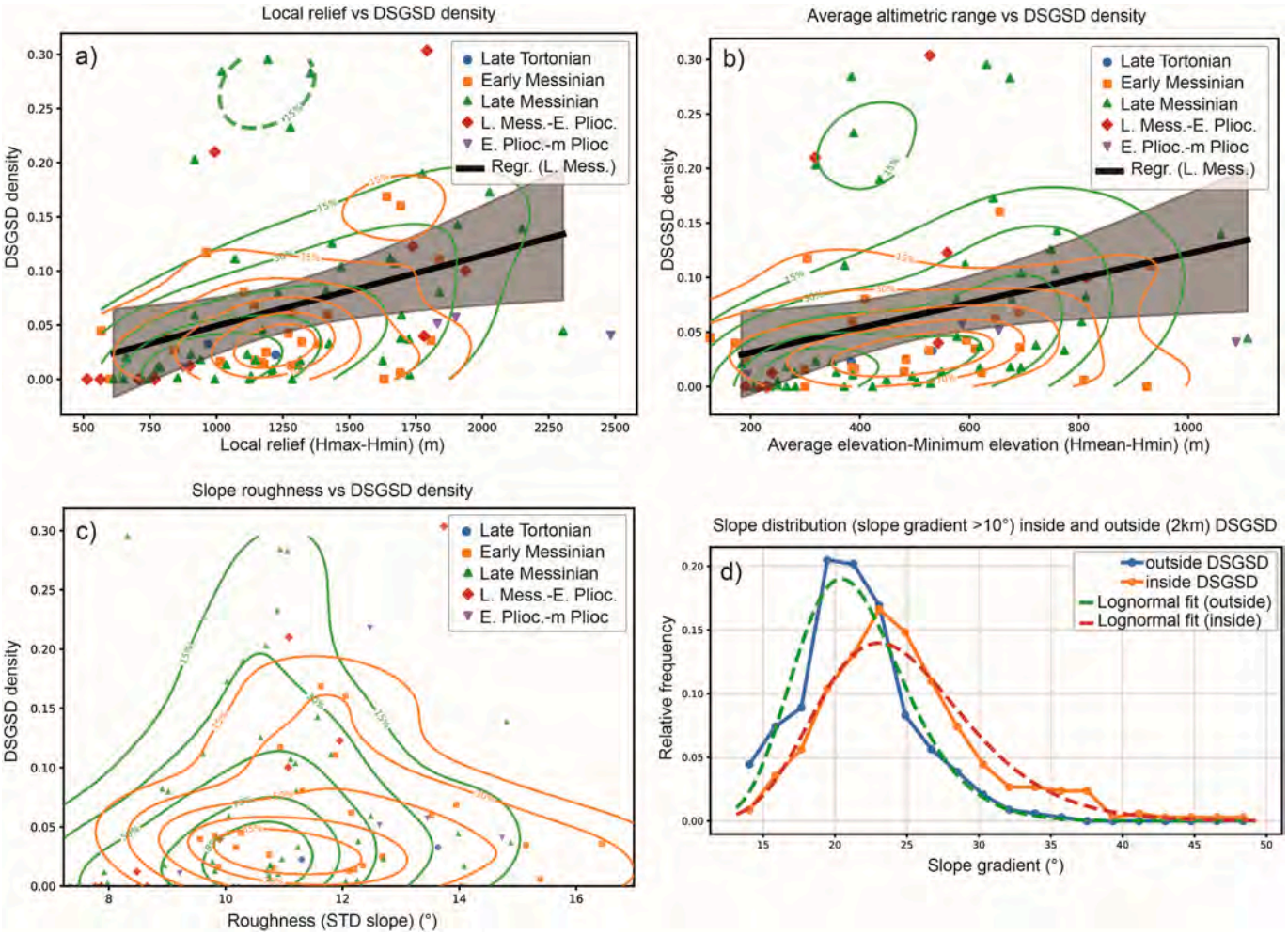


**Fig. 13.** DSGSD and bulk topography. DSGSDs density computed for the 91 squared sub-areas are plotted against: a) local relief $H_{max} - H_{min.}$; b) average altimetric range $H_{mean} - H_{min}$; c) slope roughness, i.e. standard deviation of slope gradient within 10 km wide, squared sub-area. Contour lines in panels a, b, and c indicate the kernel density distribution (KDE) of points belonging to the late Messinian (green lines) and early Messinian (orange lines) sectors of the belt; d) relative frequency of slope gradient inside and outside (2 km) DSGSD areas.

feature a limited internal elevation difference. Apart from a single DSGSDS with A > 4 km$^2$ observed in the Laga domain (Fig. 14), which is responsible for the elevated standard deviation value (Fig. 10d), other cases present a low mean areal extension (Fig. 10c).

The eastern sector of the Abruzzi region is characterized by the basin sequence and related foredeep deposits belonging to the Molise geological domain (Fig. 3). Few DSGSDs (Fig. 10a) were found, but the areal frequency for the pre-orogenic basin sequence is high (Fig. 10b). However, this is due to the limited space for outcrops, aligned in N-S elongated, narrow ridges along the eastern Abruzzi regional boundary (Di Bucci et al., 1999; Di Luzio et al., 1999) (Fig. 3). Regarding the foredeep deposits, it must be underlined the high value (2.04 km$^2$) shown by the mean area (Figs. 10c). This might be explained considering the clayey nature of the flysch terrains that are tectonically overlain by plateaus of biodetritic, calcareous and competent rocks, a geological scenario favouring the onset of large spreading processes.

In addition to the evidence of clear linear clustering and the influence of lithology, in this work we tried to unravel further factors controlling the DSGSDs density at the orogen scale. The territory of the Abruzzi region (not covered by Quaternary deposits) was divided based on the age of the first involvement in the belt structure, which occurred between the late Tortonian and the middle Pliocene. This was to understand whether the age of tectonic deformation and consequential rock damage had any type of consequence. Surprisingly, it turned out that the timing of the deformation had no influence on the distribution of DSGSD, which was controlled above all by the presence of inherited and recent structural features. However, outside the dominant phenomenon of linear clustering, it was possible to observe a relative concentration of DSGSDs in correspondence with the sector of the belt that was deformed for the first time in the late Messinian, roughly corresponding to the central-southern sector of the Gran Sasso-Genzana geological domain (Fig. 12a, b).

This evidence could be explained considering that this part of the mountain belt lies in the hanging-wall of out-of-sequence, deep stacking structures enucleated between the Middle-Late Pleistocene (Patacca et al., 2008; Di Luzio et al., 2009). The deep stacking of the Permo-Triassic section of the orogenic wedge (Figs. 4a and 12c) is hypothesized as responsible for the passive uplift and increased deformation of the overlying nappes. Stacking-related uplift would have been added to the former uplift due to in-sequence thrusting and the post-Early Pleistocene dome-like uplift of the whole Apennine belt, thus determining more favourable conditions for DSGSD onset and development.

This hypothesis seems to be confirmed if the role of bulk topography on DSGSDs density is analysed. Areas with different long-term uplift history exhibit different characteristics. Similar to other mountain belts (the Alps, Agliardi et al., 2013), high values of local relief ($H_{max} - H_{min}$) and average altimetric range ($H_{mean} - H_{min}$), paired with moderate values of slope roughness $\sigma_s$, increase DSGSD density. Actually, the

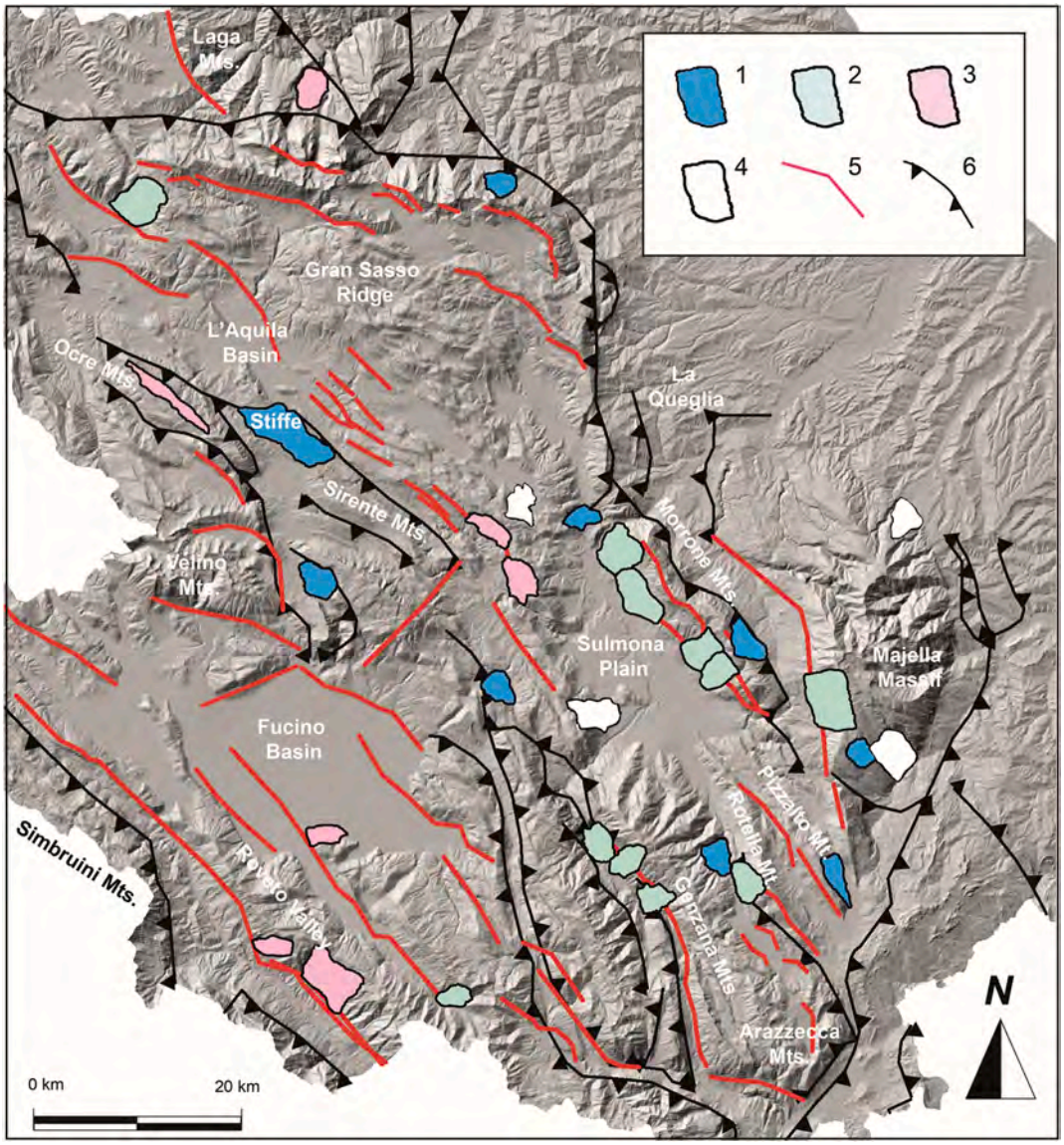


**Fig. 14.** Map distribution of DSGSDs with A > 4 km$^2$. Legend: 1) DSGSDs in forelimb zone of positive, thrust-related structure; 2) DSGSDs along backlimb sectors; 3) DSGSDs intersecting or close to Plio-Quaternary normal or transcurrent faults; 4) DSGSDs far from tectonic structures (1 km buffer); 5) Plio-Quaternary faults; 6) Mio-Pliocene thrusts.

analysis performed on the 91 sub-areas indicates that the late Messinian dataset shows the lower values of slope roughness and the higher values of local relief and average altimetric range (Fig. 13a–c). In particular, elevated $H_{mean} - H_{min}$ and moderate slope roughness outline valley incisions to local base levels in a smooth landscape. Here, slope unconfinements and stress concentrations occur along a few, deeply incised valleys. Localized uplift in the late Messinian portion of the belt, as that implied by the deep stacking, could be the reason for significant local relief and the degree of valley incisions favourable to DSGSDs.

In their turn, widespread and abundant DSGSDs played a role in the topographic settings of local reliefs. Again, following the example from Agliardi et al. (2013), this hypothesis was tested by comparing the relative frequency distribution of slope gradient inside and outside DSGSD polygons, within a 2 km buffer zone. Results are shown in Fig. 13d and, unlike evidence coming from the Alpine territory, these outline an increase in slope angle inside DSGSDs. This may be explained considering the high-resolution DEM used (10-m resolution), capable of detecting the effect on slope gradient determined by geomorphological features inside DSGSDs such as scarps, counterscarps, trenches, extended fractures, etc.. DSGSDs in the Abruzzi territory are then considered responsible for local relief rejuvenation, particularly for mature-stage DSGSDs with the presence of numerous geomorphological features.

Finally, the results of this work can be combined with the regional inventory realized by Discenza et al. (2023b) in the nearby Molise region (80 case histories). The merged geodatabase (Fig. 15) reinforces the idea that DSGSDs exhibit a regional, orogen-scale distribution and must be regarded, in all respects, as an important morphogenetic factor in landscape evolution.

Analysing the two datasets, large-scale rock slope deformations in the Molise region have a mean area ranging between 2.10 and 2.30 km$^2$ (for sackung and spreading types of DSGSDs, respectively), which is comparable to that of the Abruzzi region (1.68 km$^2$ for unclassified DSGSDs in Table 4). In addition, DSGSDs morphometric characteristics are similar, as the W/L (>1) and the H/L (about 0.4) ratios. On the one hand, this evidence confirms the validity of the analytical methods. On the other hand, and more importantly, it reveals that DSGSDs are a homogeneous geological process with similar characteristics throughout the central Apennines. The main difference between the two databases regards the mean elevation within DSGSDs, which is much lower in the

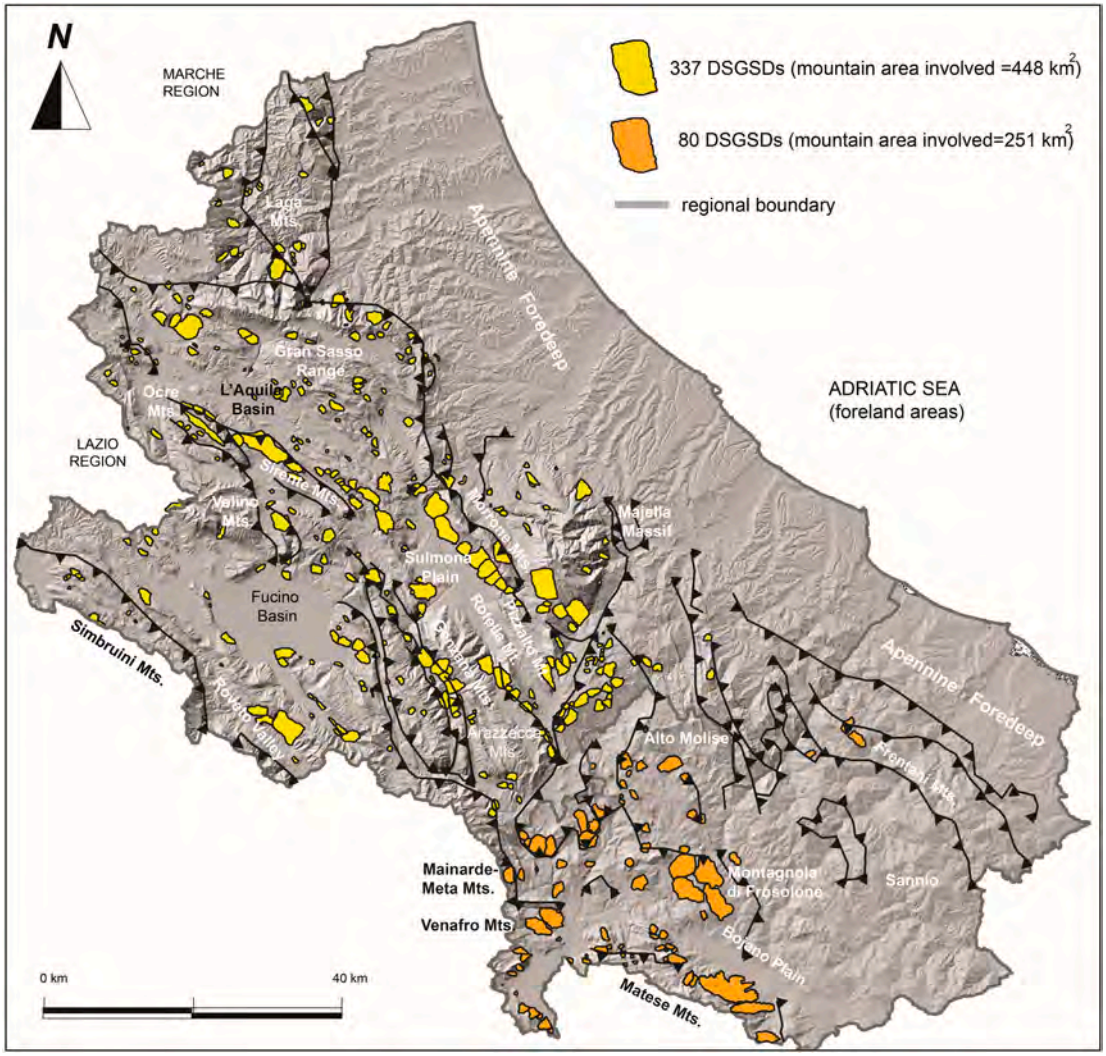


**Fig. 15.** Merged Abruzzi and Molise DSGSDs inventories (from this work and Discenza et al., 2023b, respectively). Geological structures are from Patacca et al. (2008, revisited).

Molise area (300 m vs 1100 m). The reason could be the several cases of spreading involving low-topography, rigid rocky plateaus placed on gently inclined, clayey slopes, or the highest elevation of carbonate massifs in the Abruzzi territory.

Concluding, both the Abruzzi and the Molise DSGSD inventories were created from various sources and using different types of data, mostly optical imagery. Field controls cover almost the 90% of case histories. However, it is quite likely that the inventories are not complete, and future efforts will be dedicated to dataset revision and implementation with additional case-histories.

## 6. Conclusion

Focusing on the Abruzzi region, the core of the central Apennines mountain territory, this study provides a regional inventory of DSGSDs through the analysis of 337 observed case-histories from previous databases, historical literature, and original documentation. Mapping operations were based on a geomorphological criterion. Typical surface features were enclosed in polygons through photointerpretation of aerial and satellite images supported by detailed field controls. Main results of the DSGSDs inventory outlined:

1) a widespread occurrence of DSGSDs in the mountain region (7–8% of total area), with a power law relationship between DSGSD areal extent and frequency distribution for $A > 1.01$ km$^2$;
2) linear clustering of DSGSDs along principal Neogene thrust fronts and main Plio-Quaternary normal faults.
3) exceptionally large phenomena ($A > 4$ km$^2$) found along the collapsed backlimb of main positive structures such as the Majella, Morrone, Rotella and Genzana ridges.
4) geolithological characteristics playing a key role, as DSGSDs are frequent in carbonate platform or slope-to-basin sequences, less present in siliciclastic, flysch deposits;
5) apart from linear clustering, a DSGSDs distribution which seems to be linked to the long-term history of the belt, characterized by passive uplift and deformation due to deep stacking processes (this mainly regarding the late Messinian portion of the belt);
6) bulk topography indicating high values of local relief and average altimetric range, coupled with moderate values of slope roughness, as favourable conditions for DSGSDs development (the late Messinian section of the belt best matching these requirements);
7) similar characteristics in terms of shape, size, and spatial distribution of DSGSDs, if compared to an inventory in the nearby Molise region, thus suggesting a homogenous character.

This work draws a foundational framework for future studies in the

Apennine region. Indeed, efforts will be dedicated to completing a database for the whole mountain belt. Detailed mapping represents a crucial step towards achieving a zonation of both direct and indirect DSGSD-related hazards, the former due to active deformations of large masses (even with low deformation rates), and the latter concerning potentially catastrophic landslides, as well as possible seismic amplifications.

## CRediT authorship contribution statement

**E. Di Luzio:** Writing – original draft, Visualization, Supervision, Project administration, Investigation, Funding acquisition, Formal analysis, Data curation, Conceptualization. **M. Saroli:** Writing – review & editing, Visualization, Supervision, Project administration, Methodology, Investigation, Formal analysis, Data curation, Conceptualization. **M. Moro:** Writing – review & editing, Visualization, Supervision, Software, Project administration, Investigation, Formal analysis, Data curation, Conceptualization. **E. Zullo:** Writing – review & editing, Validation, Software, Methodology, Data curation. **M. Albano:** Writing – review & editing, Validation, Software, Methodology, Data curation. **G. Scarascia Mugnozza:** Writing – review & editing, Supervision, Project administration, Investigation, Conceptualization. **M.E. Discenza:** Writing – review & editing, Validation, Formal analysis, Data curation, Conceptualization. **M. Fiorucci:** Visualization, Software, Investigation. **D. Guglietta:** Methodology, Investigation, Data curation, Conceptualization. **C. Esposito:** Writing – review & editing, Supervision, Project administration, Investigation, Funding acquisition, Formal analysis, Conceptualization.

## Fundings

This work was financed by the CNR Project “Apennine Gravitational Processes” (code DTA.AD003.731.001, resp. Dr. Emiliano Di Luzio) and partially supported by funds from Sapienza University project “Integrated analysis and hazard-oriented modelling of large-scale slope instabilities featured by Mass Rock Creep” (prot. RG11916B88FA477F; resp. Prof. Carlo Esposito).

## Declaration of competing interest

The authors declare that they have no known competing financial interests or personal relationships that could have appeared to influence the work reported in this paper.

## Acknowledgements

Authors are grateful to Prof. Pierluigi Pieruccini (University of Turin) for his advice on the DSGSD in the Stiffe area and in the Laga domain, and to Dr. Valensise G. (INGV) for his support in the initial stage of this research. We thank Dr. Sergio Falcone for the development of the code used for the stereoscopic visualization and analysis (available at: https://zenodo.org/badge/latestdoi/546700017, accessed on 12 April 2025). Contribution in the field by Bianchi Fasani G.L. (ENEA) and more recently by Marmoni G.M. and Khalaf, N. H. M. (both Sapienza University of Rome) were appreciated. Finally, the Authors acknowledge the valuable contribution offered by two anonymous reviewers to improve the quality of the paper.

## Data availability

The data that has been used is confidential.

## References

Agliardi, F., Crosta, G.B., Zanchi, A., 2001. Structural constraints on deep-seated slope deformation kinematics. Eng. Geol. 59, 83–102. https://doi.org/10.1016/S0013-7952(00)00066-1.

Agliardi, F., Crosta, G.B., Frattini, P., 2012. Slow rock-slope deformation. In: Clague, J.J., Stead, D. (Eds.), Landslides: Types, Mechanisms and Modeling. Cambridge University Press, Cambridge, pp. 207–221. https://doi.org/10.1017/CBO9780511740367.019.

Agliardi, F., Crosta, G.B., Frattini, P., Malusà, M.G., 2013. Giant non-catastrophic landslides and the long-term exhumation of the European Alps. Earth Planet. Sci. Lett. 365, 263–274. https://doi.org/10.1016/j.epsl.2013.01.030.

Albano, M., Barba, S., Saroli, M., Moro, M., Malvarosa, F., Costantini, M., Bignami, C., Stramondo, S., 2015. Gravity-driven postseismic deformation following the Mw 6.3 2009 L'Aquila (Italy) earthquake. Sci. Rep. 5, 16558. https://doi.org/10.1038/srep16558.

Albano, M., Saroli, M., Beccaro, L., Moro, M., Doumaz, F., Discenza, M.E., Del Rio, L., Rompato, M., 2023. Multi-source data analysis to assess the past and present kinematics of the Pisciotta Deep-Seated Gravitational Slope Deformation (southern Italy). Remote Sens. Environ. 296, 11375. https://doi.org/10.1016/j.rse.2023.113751.

Allen, S.K., Cox, S.C., Owens, I.F., 2011. Rock avalanches and other landslides in the central Southern Alps of New Zealand: a regional study considering possible climate change impacts. Landslides 8, 33–48. https://doi.org/10.1007/s10346-010-0222-z.

Ambrosetti, P., Carraro, F., Deiana, G., Dramis, F., 1982. Il sollevamento dell'Italia centrale tra il Pleistocene inferiore ed il Pleistocene medio. In: Contributi preliminari alla realizzazione della Carta Neotettonica d'Italia. CNR, Progetto Finalizzato Geodinamica, pp. 219–223. Publ. N°513.

Ambrosi, C., Crosta, G.B., 2006. Large sackung along major tectonic features in the Central Italian Alps. Eng. Geol. 83, 183–200. https://doi.org/10.1016/j.enggeo.2005.06.031.

Ambrosi, C., Crosta, G.B., 2011. Valley shape influence on deformation mechanisms of rock slopes. Geol. Soc. Lond. Spec. Publ. 351, 215–233.

Bartolini, C., D'Agostino, N., Dramis, F., 2003. Topography, exhumation and drainage network evolution of the Apennines. Episodes 26, 212–216. https://doi.org/10.18814/epiiugs/2003/v26i3/010.

Bianchi Fasani, G., Di Luzio, E., Esposito, C., Martino, S., Scarascia Mugnozza, G., 2011. Numerical modeling of Plio-Quaternary slope evolution based on geological constraints: a case study from the Caramanico Valley (central Apennines, Italy). Geol. Soc. Lond. Spec. Publ. 351, 201–214. https://doi.org/10.1144/sp351.11.

Bianchi Fasani, G., Di Luzio, E., Esposito, C., Evans, S.G., Scarascia Mugnozza, G., 2014. Quaternary, catastrophic rock avalanches in the Central Apennines (Italy): relationships with inherited tectonic features, gravity-driven deformations and the geodynamic frame. Geomorphology 211, 22–42. https://doi.org/10.1016/j.geomorph.2013.12.027.

Billi, A., Tiberti, M.M., Cavinato, G.P., Cosentino, D., Di Luzio, E., Keller, J.V.A., Kluth, C., Orlando, L., Parotto, M., Praturlon, A., Romanelli, M., Storti, F., Wardell, N., 2006. First results from the CROP-11 deep seismic profile, central Apennines, Italy: evidence of mid-crustal folding. J. Geol. Soc. Lond. 163 (4), 583–586. https://doi.org/10.1144/0016-764920-002.

Bovis, 1982. Uphill-facing (antislope) scarps in the Coast Mountains, southwest British Columbia. Geol. Soc. Am. Bull. 93, 804–812.

Carminati, E., Doglioni, C., 2012. Alps vs. Apennines: the paradigm of a tectonically asymmetric Earth. Earth Sci. Rev. 112 (1–2)), 67–96. https://doi.org/10.1016/j.earscirev.2012.02.004.

Cavinato, G.P., De Celles, P.G., 1999. Extensional basins in the tectonically bimodal central Apennines fold-thrust belt, Italy: response to corner flow above a subducting slab in retrograde motion. Geology 27 (10), 955–958. https://doi.org/10.1130/0091-7613(1999)027<0955: EBITTB>2.3.CO;2.

Cavinato, G.P., Carusi, C., Dall'Asta, M., Miccadei, E., Piacentini, T., 2002. Sedimentary and tectonic evolution of Plio-Pleistocene alluvial and lacustrine deposits of Fucino Basin (central Italy). Sediment. Geol. 148 (1–2), 29–59. https://doi.org/10.1016/S0037-0738(01)00209-3.

Centamore, E., Nisio, S., 2003. Effects of uplift and tilting in the central-northern Apennines (Italy). Quat. Int. 101–102, 93–101. https://doi.org/10.1016/S1040-6182(02)00092-7.

Chigira, M., 1992. Long-term gravitational deformation of rocks by mass rock creep. Eng. Geol. 32, 157–184.

Cosentino, D., Cipollari, P., Marsili, P., Scrocca, D., 2010. Geology of the central Apennines: a regional review. In: Beltrando, M., Peccerillo, A., Mattei, M., Ponticelli, S., Dogliosi, C. (Eds.), The Geology of Italy, Journal of the Virtual Explorer, Vol. 36. https://doi.org/10.3809/jvirtex.2010.00223.

Crescenti, U., Dramis, F., Gentili, B., Pambianchi, G., 1987. Deformazioni gravitative profonde di versante e grandi frane nell'area a Sud di Monte Porrara (Appennino centrale, Abruzzo). Mem. Soc. Geol. Ital. 39, 477–486.

Crosta, G., 1996. Landslide, spreading, deep seated gravitational deformation: analysis, examples, problems and proposals. Geogr. Fis. Din. Quat. 19, 297–313.

Crosta, G.B., Frattini, P., Agliardi, F., 2013. Deep seated gravitational slope deformations in the European Alps. Tectonophysics 605, 13–33. https://doi.org/10.1016/j.tecto.2013.04.028.

D'Agostino, N., Jackson, J.A., Dramis, F., Funiciello, R., 2001. Interactions between mantle upwelling, drainage evolution and active normal faulting: an example from the central Apennines (Italy). Geophys. J. Int. 147, 475–497. https://doi.org/10.1046/j.1365-246X.2001.00539.x.

Del Rio, L., Moro, M., Fondriest, M., Saroli, M., Gori, S., Falcucci, E., Cavallo, A., Doumaz, F., Di Toro, G., 2021. Active faulting and deep-seated gravitational slope

deformation in carbonate rocks (central Apennines, Italy): a new “close-up” view. Tectonics 40. https://doi.org/10.1029/2021TC006698 e2021TC006698.
Delchiaro, M., Mele, E., Della Seta, M., Martino, S., Mazzanti, P., Esposito, C., 2021. Quantitative investigation of a mass rock creep deforming slope through A-Din SAR and geomorphometry. In: Vilímek, V., Wang, F., Strom, A., Sassa, K., Bobrowsky, P. T., Takara, K. (Eds.), Understanding and Reducing Landslide Disaster Risk. WLF 2020, ICL Contribution to Landslide Disaster Risk Reduction. Springer, Cham. https://doi.org/10.1007/978-3-030-60319-9_18.
Della Seta, M., Esposito, C., Marmoni, G.M., Martino, S., Scarascia Mugnozza, G., Troiani, F., 2017. Morpho-structural evolution of the valley-slope systems and related implications on slope-scale gravitational processes: new results from the Mt. Genzana case history (Central Apennines). Geomorphology 289, 60–77. https://doi.org/10.1016/j.geomorph.2016.07.003.
Di Bucci, D., Corrado, S., Naso, G., Parotto, M., Praturlon, A., 1999. Evoluzione tettonica neogenico-quaternaria dell’area molisana. Ital. J. Geosci. 118 (1), 13–30.
Di Luzio, E., Paniccia, D., Pitzianti, P., Sansonne, P., Tozzi, M., 1999. Evoluzione tettonica dell’Alto Molise. Ital. J. Geosci. 118 (2), 287–315.
Di Luzio, E., Saroli, M., Esposito, C., Bianchi Fasani, G., Cavinato, G.P., Scarascia, Mugnozza G., 2004a. Influence of structural framework on mountain slope deformation in the Maiella anticline (Central Apennines, Italy). Geomorphology 60, 417–432. https://doi.org/10.1016/j.geomorph.2003.10.004.
Di Luzio, E., Bianchi-Fasani, G., Esposito, C., Saroli, M., Cavinato, G.P., Scarascia-Mugnozza, G., 2004b. Massive rock-slope failure in the Central Apennines (Italy): the case of the Campo di Giove rock avalanche. Bull. Eng. Geol. Environ. 63, 1–12. https://doi.org/10.1007/s10064-003-0212-7.
Di Luzio, E., Mele, G., Tiberti, M.M., Cavinato, G.P., Parotto, M., 2009. Moho deepening and shallow upper crustal delamination beneath the central Apennines. Earth Planet. Sci. Lett. 280 (1–4), 1–12. https://doi.org/10.1016/j.epsl.2008.09.018.
Di Luzio, E., Schilirò, L., Gaudiosi, I., 2021. Cultural heritage and rockfalls: analysis of multi-scale processes nearby the *Lucus Angitiae* archaeological site (Central Italy). Geosciences 11, 521. https://doi.org/10.3390/geosciences11120521.
Di Luzio, E., Discenza, M.E., Di Martire, D., Putignano, M.L., Minnillo, M., Esposito, C., Scarascia Mugnozza, G., 2022. Investigation of the Luco dei Marsi DSGSD revealing the first evidence of a basal shear zone in the Central Apennine belt (Italy). Geomorphology 408, 108249. https://doi.org/10.1016/j.geomorph.2022.108249.
Discenza, M.E., Esposito, C., 2021. State-of-art and remarks on some open questions about DSGSDs: hints from a review of the scientific literature on related topics. Ital. J. Eng. Geol. Environ. 21 (1), 31–59. https://doi.org/10.4408/IJEGE.2021-01.O-03.
Discenza, M.E., Esposito, C., Martino, S., Petitta, M., Prestininzi, A., Scarascia Mugnozza, G., 2011. The gravitational slope deformation of Mt. Rocchetta ridge (central Apennines, Italy): geological-evolutionary model and numerical analysis. Bull. Eng. Geol. Environ. 70 (4), 559–575. https://doi.org/10.1007/S10064-010-0342-7.
Discenza, M.E., Di Luzio, E., Martino, S., Minnillo, M., Esposito, C., 2023a. Role of inherited tectonic structures on gravity-induced slope deformations: inference from numerical modeling on the Luco dei Marsi DSGSD (Central Apennines). Appl. Sci. 13 (7), 4417. https://doi.org/10.3390/app13074417.
Discenza, M.E., Esposito, C., Di Luzio, E., Delchiaro, M., Di Martire, D., Minnillo, M., Scarascia Mugnozza, G., 2023b. Deep-seated gravitational slope deformations in Molise region (Italy): novel inventory and main geomorphological features. J. Maps 19 (1), 2163198. https://doi.org/10.1080/17445647.2022.2163198.
Doglioni, C., 1991. A proposal for the kinematic modelling of W-dipping subductions — possible applications to the Tyrrhenian-Apennines system. Terra Nova 3, 423–434. https://doi.org/10.1111/j.1365-3121.1991.tb00172.x.
Dramis, F., 1992. Il ruolo dei sollevamenti tettonici a largo raggio nella genesi del rilievo appenninico. Stud. Geol. Cam. 1992 (1), 9–15.
Dramis, F., Sorriso-Valvo, M., 1994. Deep-seated gravitational slope deformations, related landslides and tectonics. Eng. Geol. 38, 231–243. https://doi.org/10.1016/0013-7952(94)90040-X.
Dramis, F., Gentili, B., Pambianchi, G., 1987. Deformazioni gravitative profonde nell'area di Monte Gorzano (Monti della Laga, Appennino Centrale). Boll. Soc. Geol. It. 106, 265–271.
Esposito, C., Martino, S., Scarascia Mugnozza, G., 2007. Mountain slope deformations along thrust fronts in jointed limestone: an equivalent continuum modelling approach. Geomorphology 90, 55–72. https://doi.org/10.1016/j.geomorph.2007.01.017.
Esposito, C., Bianchi Fasani, G., Martino, S., Scarascia Mugnozza, G., 2013. Quaternary gravitational morpho-genesis of central Apennines (Italy): insights from the Mt Genzana case history. Tectonophysics 605, 96–103. https://doi.org/10.1016/j.tecto.2013.06.023.
Esposito, C., Di Luzio, E., Baleani, M., Troiani, F., Della Seta, M., Bozzano, F., Mazzanti, P., 2021. Fold architecture predisposing deep-seated gravitational slope deformations within a flysch sequence in the Northern Apennines (Italy). Geomorphology 380, 107629. https://doi.org/10.1016/j.geomorph.2021.107629.
Esposito, C., Di Luzio, E., Scarascia Mugnozza, G., Bianchi Fasani, G., 2014. Mutual interactions between slope-scale gravitational processes and morpho-structural evolution of central Apennines (Italy): review of some selected case histories. Rend. Lincei 25, 151–165. https://doi.org/10.1007/s12210-014-0348-3.
Faccenna, C., Davy, P., Brun, J.P., Funiciello, R., Giardini, D., Mattei, M., Nalpas, T., 1996. The dynamics of back-arc extension: an experimental approach to the opening of the Tyrrhenian Sea. Geophys. J. Int. 126 (3), 781–795. https://doi.org/10.1111/j.1365-246X.1996.tb04702.x.
Frattini, P., Crosta, G.B., Allievi, J., 2013. Damage to buildings in large slope rock instabilities monitored with the PSInSAR™ technique. Remote Sens. 5, 4753–4773. https://doi.org/10.3390/rs5104753.
Galadini, F., 2006. Quaternary tectonics and large-scale gravitational deformations with evidence of rock-slide displacements in the Central Apennines (Central Italy). Geomorphology 82, 201–228. https://doi.org/10.1016/j.geomorph.2006.05.003.
Galadini, F., Galli, P., 2000. Active tectonics in the central Apennines (Italy) — input data for seismic hazard assessment. Nat. Hazards 22, 225–268. https://doi.org/10.1023/A:1008149531980.
Galadini, F., Messina, P., 1994. Plio-Quaternary tectonics of the Fucino basin and surrounding areas (Central Italy). Gior. Geol. Ser. 3 56 (2), 73–99.
Galadini, F., Messina, P., Giaccio, B., Sposato, A., 2003. Early uplift history of the Abruzzi Apennines (central Italy): available geomorphological constraints. Quat. Int. 101–102, 125–135. https://doi.org/10.1016/S1040-6182(02)00095-2.
Galli, G., Galadini, F., Pantosti, D., 2008. Twenty years of paleoseismology in Italy. Earth Sci. Rev. 88 (1–2), 89–117. https://doi.org/10.1016/j.earscirev.2008.01.001.
Gori, S., Falcucci, E., Dramis, F., Galadini, F., Galli, P., Giaccio, B., Messina, P., Pizzi, A., Sposato, A., Cosentino, D., 2014. Deep-seated gravitational slope deformation, large-scale rock failure, and active normal faulting along Mt. Morrone (Sulmona basin, central Italy): Geomorphological and paleoseismological analyses. Geomorphology 208, 88–101. https://doi.org/10.1016/j.geomorph.2013.11.017.
Gori, S., Falcucci, E., Ladina, C., Marzorati, S., Galadini, F., 2017. Active faulting, 3-D geological architecture and Plio-Quaternary structural evolution of extensional basins in the central Apennine chain, Italy. Solid Earth 8 (2), 319–337. https://doi.org/10.5194/se-8-319-2017.
Gueguen, E., Doglioni, C., Fernandez, M., 1998. On the post-25 Ma geodynamic evolution of the western Mediterranean. Tectonophysics 298 (1–3), 259–269. https://doi.org/10.1016/S0040-1951(98)00189-9.
IFFI, 2007. Report on landslides in Italy: the IFFI project. Methodology, results and regional reports. APAT Rep. 78, 681.
Jaboyedoff, M., Crosta, G.B., Stead, D., 2011. Slope tectonics: a short introduction. Geol. Soc. Lond. Spec. Publ. 351, 1–10. https://doi.org/10.1144/SP351.1.
Jaboyedoff, M., Penna, I., Pedrazzini, A., Baron, I., Crosta, G.B., 2013. An introducing review on gravitational-deformation induced structures, fabrics and modeling. Tectonophysics 605, 1–12. https://doi.org/10.1016/j.tecto.2013.06.027.
Jarman, D., 2006. Large rock slope failures in the Highlands of Scotland: characterisation, causes and spatial distribution. Eng. Geol. 83, 161–182. https://doi.org/10.1016/j.enggeo.2005.06.030.
Jarman, D., Harrison, S., 2019. Rock slope failure in the British Mountains. Geomorphology 340, 202–233. https://doi.org/10.1016/j.geomorph.2019.03.002.
Jarman, D., Calvet, M., Corominas, J., Delmas, M., Gunnell, Y., 2014. Large-scale rock slope failures in the Eastern Pyrenees: identifying a sparse but significant population in paraglacial and parafluvial contexts. Geogr. Ann. Ser. B 96, 357–391. https://doi.org/10.1111/geoa.12060.
Jaurand, E., 1999. Il glacialismo negli Appennini. Boll. Soc. Geogr. Ital. 12 (4), 399–432.
Kaneda, H., Kono, T., 2017. Discovery, controls, and hazards of widespread deep-seated gravitational slope deformation in the Etsumi Mountains, central Japan. J. Geophys. Res.: Earth Surf. 122, 2370–2391. https://doi.org/10.1002/2017JF004382.
Khalaf, N.H.M., Di Luzio, E., Scarascia Mugnozza, G., Esposito, C., Saroli, M., Moro, M., Marmoni, G.M., Giannini, L.M., Fiorucci, M., Doumaz, F., 2025. Geological model of the Stiffe-San Martino d'Ocre ridge (central Apennines, Italy); evidence of multiple factors driving a mountain-scale deformation. Ital. J. Eng. Geol. Environ. 2, 61–75. https://doi.org/10.4408/IJEGE.2024-02.O-06.
Malgot, J., 1977. Deep-seated gravitational slope deformations in neovolcanic mountain ranges of Slovakia. Bull. Int. Assoc. Eng. Geol. 16, 106–109.
Malinverno, A., Ryan, W.B.F., 1986. Extension in the Tyrrhenian Sea and shortening in the Apennines as a result of the arc migration driven by sinking of the lithosphere. Tectonics 5 (2), 227–245.
Martino, S., Prestininzi, A., Scarascia Mugnozza, G., 2004. Geological-evolutionary model of a gravity-induced slope deformation in the carbonate central Apennines (Italy). Q. J. Eng. Geol. Hydrogeol. 37, 31–47. https://doi.org/10.1144/1470-9236/03-030.
McLean, M.C., Brideau, M.A., Augustinus, P.C., 2015. Deep-seated gravitational slope deformation in greywacke rocks of the Tararua Range, North Island, New Zealand. In: Lollino, G., Giordan, D., Crosta, G.B., Corominas, J., Azzam, R., Wasowski, J., Sciarra, N. (Eds.), Engineering Geology for Society and Territory, vol. 2. Springer, pp. 559–564. https://doi.org/10.1007/978-3-319-09057-3_92.
Moro, M., Saroli, M., Tolomei, C., Salvi, S., 2009. Insights on the kinematics of deep-seated gravitational slope deformations along the 1915 Avezzano earthquake fault (central Italy), from time-series DInSAR. Geomorphology 112, 261–276. https://doi.org/10.1016/j.geomorph.2009.06.011.
Moro, M., Chini, M., Saroli, M., Atzori, S., Stramondo, S., Salvi, S., 2011. Analysis of large, seismically induced, gravitational deformations imaged by high-resolution COSMO-SkyMed synthetic aperture radar. Geology 39 (6), 527–530. https://doi.org/10.1130/G31748.1.
Moro, M., Saroli, M., Gori, S., Falcucci, E., Galadini, F., Messina, P., 2012. The interaction between active normal faulting and large-scale gravitational mass movements revealed by paleoseismological techniques: a case study from central Italy. Geomorphology 151–152, 164–174. https://doi.org/10.1016/j.geomorph.2012.01.026.
Pánek, T., Klimeš, J., 2016. Temporal behaviour of deep-seated gravitational slope deformations: a review. Earth Sci. Rev. 156, 14–38. https://doi.org/10.1016/j.earscirev.2016.02.007.
Pànek, T., Brezny, M., Kapustova, V., Lenart, J., Chalupa, V., 2019. Large landslides and deep-seated gravitational slope deformation in Czech Flysch Carpathians: new LiDAR-based inventory. Geomorphology 346, 106852. https://doi.org/10.1016/j.geomorph.2019.106852.
Patacca, E., Scandone, P., 1989. Post-Tortonian mountain building in the Apennines: the role of the passive sinking of a relic lithospheric slab. In: Boriani, A., Bonafede, M.,

Piccardo, G.B., Vai, G.B. (Eds.), The Lithosphere in Italy, Atti Conv. Lincei, Vol. 80, pp. 157–176.
Patacca, E., Sartori, R., Scandone, P., 1990. Tyrrhenian Basin and Apenninic Arcs: Kinematic Relations since late Tortonian Times. Mem. Soc. Geol. Ital. 45, 425–451.
Patacca, E., Scandone, P., Bellatalla, M., Perilli, N., Santini, U., 1991. La zona di giunzione tra l'arco appenninico settentrionale e l'arco appenninico meridionale nell'Abruzzo e nel Molise, in: Tozzi, M., Cavinato, G.P. Parotto, M., (Eds.), Studi Preliminari all'acquisizione dati del Profilo CROP 11 "Civitavecchia-Vasto", Stud. Geol. Camerti. Spec. Vol. 1991 (2), 417–441.
Patacca, E., Scandone, P., Di Luzio, E., Cavinato, G.P., Parotto, M., 2008. Structural architecture of the central Apennines. Interpretation of the CROP 11 seismic profile from the Adriatic coast to the orographic divide. Tectonics 27, TC3006. https://doi.org/10.1029/2005TC001917.
Pizzi, A., 2003. Plio-Quaternary uplift rates in the outer zone of the central Apennines fold-and-thrust belt, Italy. Quat. Int. 101-102, 229–237. https://doi.org/10.1016/S1040-6182(02)00105-2.
Radbruch-Hall, D., 1978. Gravitational creep of rock masses slopes. Geotechnical Engineering, 14, 607–658. In: Voight, B. (Ed.), Rockslides and Avalanches Natural Phenomena. Devel, Geotechnol. Eng. 14, Vol. 17. Elsevier, Amsterdam, pp. 607–657.
Saroli, M., Stramondo, S., Moro, M., Doumaz, F., 2005. Movements detection of deep seated gravitational slope deformations by means of InSAR data and photogeological interpretation: northern Sicily case study. Terra Nova 17 (1), 35–43. https://doi.org/10.1111/j.1365-3121.2004.00581.x.
Savage, W.Z., Varnes, D.J., 1987. Mechanics of gravitational spreading of steep-sides ridges (sackung). Bull. Int. Assoc. Eng. Geol. 35, 31–36.
Scarascia Mugnozza, G., Bianchi Fasani, G., Esposito, C., Martino, S., Saroli, M., Di Luzio, E., Evans, S.G., 2006. Rock avalanche and mountain slope deformation in a convex dip-slope: the case of the Maiella massif, Central Italy. In: Evans, S.G., Scarascia Mugnozza, G., Strom, A., Hermanns, R. (Eds.), Massive Rock Slope Failure, NATO Science Series, Vol. 49. Springer, Dordrecht, pp. 357–376. https://doi.org/10.1007/978-1-4020-4037-5_19.
Stramondo, S., Trasatti, E., Albano, M., Moro, M., Chini, M., Bignami, C., Polcari, M., Saroli, M., 2016. Uncovering deformation processes from surface displacements. J. Geodyn. 102, 58–82. https://doi.org/10.1016/j.jog.2016.08.001.
Tarquini, S., Isola, I., Favalli, M., Mazzarini, F., Bisson, M., Pareschi, M.T., Boschi, E., 2007. TINITALY/01: a new triangular irregular network of Italy. Ann. Geophys. 50, 407–425. https://doi.org/10.4401/ag-4424. https://www.tinitaly.pi.ingv.it/.
Toločka, A., 2025. Towards understanding the global distribution of deep-seated gravitational deformations: a study of geological influences and spatial patterns. Nat. Hazards. https://doi.org/10.1007/s11069-025-07448-0 published online June 2025.
Tsou, C.Y., Chigira, M., Matsushi, Y., Chen, S.C., 2015. Deep-seated gravitational deformation of mountain slopes caused by river incision in the Central Range, Taiwan: spatial distribution and geological characteristics. Eng. Geol. 196, 126–138. https://doi.org/10.1016/j.enggeo.2015.07.005.
Vezzani, L., Festa, A., Ghisetti, F.C., 2010. Geology and tectonic evolution of the central-southern Apennines, Italy. Geol. Soc. Am. 469. https://doi.org/10.1130/SPE469.